Geophysical Journal International

Geophys. J. Int. (2010) **182,** 183–202 doi: 10.1111/j.1365-246X.2010.04620.x

The North Atlantic Igneous Province reconstructed and its relation to the Plume Generation Zone: the Antrim Lava Group revisited

M. Ganerød,[1,2] M. A. Smethurst,[1] T. H. Torsvik,[1,3] T. Prestvik,[2] S. Rousse,[4] C. McKenna,[5] D. J. J. van Hinsbergen[1,3] and B. W. H. Hendriks[1]

[1]*Geological Survey of Norway (NGU),* 7491 *Trondheim, Norway. E-mail: morgan.ganerod@ngu.no*
[2]*Department of Geology and Mineral Resources Engineering, Norwegian University of Science and Technology,* 7491 *Trondheim, Norway*
[3]*Physics of Geological Processes (PGP), University of Oslo,* 0316 *Oslo, Norway*
[4]*LMTG – UMR* 5563 *UR* 154 *CNRS Université Paul-Sabatier IRD Observatoire Midi-Pyrénées, Toulouse, France*
[5]*Department of Geology, University College Cork, Cork, Ireland*

Accepted 2010 April 7. Received 2010 April 7; in original form 2009 October 5

SUMMARY

Large igneous provinces (LIPs) have recently been suggested to originate at the edges of low-velocity zones on the core mantle boundary (Plume Generation Zones). If true, LIPs can potentially be used to constrain paleolongitude in plate tectonic reconstructions. To validate the hypothesis, it is essential to study LIPs of which the paleolongitude can be constrained by other methods, such as hotspot reference frames. An ideal candidate to this end is the early Cenozoic North Atlantic Igneous Province (NAIP). Despite being the largest volcanic unit of the British Tertiary Igneous Province (BTIP, part of the NAIP), the age and paleoposition of the Antrim Lava Group (ALG) in Northern Ireland, which is key to the NAIP as a whole, was hitherto poorly constrained. In this paper, we therefore present an integrated high-resolution paleomagnetic and geochronological study.

The ALG is divided into three formations: the Lower Basalt Formation (LBF), Interbasaltic Formation (IBF) and the Upper Basalt Formation (UBF). The IBF is mostly lateritic and encloses the Tardree rhyolite. We offer new age constraints from all three formations using the $^{40}Ar/^{39}Ar$ method and propose that 62.6 ± 0.3, 61.3 ± 0.3 and 59.6 ± 0.3 Ma (1σ, internal uncertainties) are sound estimates of the age of emplacement of the LBF, Tardree rhyolite (IBF) and UBF, respectively. This constrains the nominal duration of emplacement of the ALG to 3 ± 0.6 Ma (1σ).

This reevaluation of the magnetic signature in the ALG revealed reverse polarity remanence in all three formations and an overall paleomagnetic north pole at latitude 78.9°N, longitude 167°E (A95 = 6.3; age ∼61 Ma) in the European reference system. This appears consistent with paleomagnetic poles from the rest of the NAIP; both in Europe and Greenland, as well as predictions from modern apparent polar wander paths.

The new radiometric ages span magnetochron C26r, C27n and C27r. The normal polarity chron C27n most probably occurred during the IBF hiatus, explaining why no normal polarity remanence was detected in the paleomagnetic investigation. Emplacement of the LBF falls in magnetochron C27r, making this one of the oldest lava sequence in the NAIP; older than the C27n lava pile in Western Greenland.

The 60 Ma position of the NAIP in a paleomagnetic reference frame, puts it close to the northern edge of the African large low shear wave velocity anomaly at the core–mantle boundary and therefore in the line with the Plume Generation Zone hypothesis. However, the back-projected Icelandic hotspot, normally considered to have formed the NAIP, is located ∼1500 km north of the latitude at which the NAIP erupted. The northward motion of the north Atlantic lithosphere since the late Cretaceous challenging the existing correlation of the NAIP to the Icelandic hotspot, normally used to explain the observed pre- and syn-breakup North Atlantic magmatism (63–55 Ma), and either an additional plume located further south in the North Atlantic may be invoked to create the NAIP, or the Icelandic hotspot must have undergone a northward motion together with the North Atlantic lithosphere (which according to present mantle flow models seems unlikely).

Key word: Magnetostratigraphy; Palaeomagnetism applied to geologic processes; Hotspots; Large igneous provinces.

INTRODUCTION

Large igneous provinces (LIPs) have been associated with the rifting of continents (Courtillot *et al.* 1999), initiated by deep-seated mantle plumes (Burke *et al.* 2008) or other mechanism (e.g. King & Anderson 1998), both poorly understood. Recently, Torsvik *et al.* (2006) and Burke *et al.* (2008) postulated that LIPs over the past 300 Ma were almost exclusively derived from the margins (the Plume Generation Zone, PGZ) of two antipodal zones on the core–mantle boundary, known as the large low shear velocity provinces (LLSVPs). Torsvik *et al.* (2008b) proposed that with their age and paleolatitude known, LIPs can be used to constrain paleolongitudes of plates in times where no alternative methods (such as hotspot reference frames or ocean floor anomalies) can be applied.

One of the many known LIPs (Mahoney & Coffin 1997) developed in the Tertiary proto North Atlantic during the final rifting of Pangea where the massive piles of continental flood basalt making up the North Atlantic Igneous Province (NAIP) can be found (Fig. 1a). The NAIP was split in two by the opening of the North Atlantic and its principal components are now widely distributed and exposed in East and West Greenland, on the Faeroe Islands and in the British Isles (Saunders *et al.* 1997). Most of the British Tertiary igneous province (BTIP), a subprovince of NAIP, crops out in Antrim (Northern Ireland) and on the Isles of Mull and Skye in Scotland (Fig. 1b, Saunders *et al.* 1997). The origin of LIPs is still hotly debated and a review of different models for the development of NAIP can be found in Meyer *et al.* (2007).

To test whether the NAIP was generated in the PGZ, our principal interests in the NAIP are twofold. First, we want to establish the time window of emplacement of the vast Antrim lava sequence, to put the Antrim lavas in their correct place in the eruption history of the BTIP and NAIP, and secondly to determine whether the paleomagnetic pole position for the Antrim lavas is consistent with pole positions derived from the rest of the NAIP. Regarding our first ambition, we have gathered all relevant radiometric age determinations for the Antrim lava sequences in the literature and have supplemented these with new $^{40}Ar/^{39}Ar$ ages. As well as sampling for radiometric dating, we also carried out a comprehensive sampling campaign for paleomagnetic study with an objective to further refine our knowledge of the magnetic reversal stratigraphy of the lava pile. The radiometric ages and magnetic stratigraphy together let us anchor the lava sequence to specific magnetochrons in the global polarity timescale.

GEOLOGICAL SETTING

Stratigraphy

The Antrim plateau in Northern Ireland hosts the largest remnants of the BTIP (Fig. 1c). Volcanic activity started with sporadic explosive eruptions in the North resulting in the formation of ash cones, vent agglomerates and pyroclastic tuffs, followed by flooding of carstified early Upper Mastrichtian limestones (Simms 2000; Mitchell 2004) by the Antrim Lava Group (ALG; Fig. 2a). The ALG was produced in two major cycles represented by the Lower Basalt Formation (LBF) and Upper Basalt Formation (UBF, Old 1975). The predominantly hyperstene normative basalts of the LBF and UBF are separated by up to 30 m of laterites belonging to the Interbasaltic Formation (IBF; Fig. 2a) representing a considerable time of dormancy and weathering (Hill *et al.* 2000). This time of dormancy was interrupted in the north by extrusion of the quartz-tholeiitic Causeway Member (CM) of the IBF. The CM is 150 m thick in total and consists of up to nine thick flows exhibiting spectacular columnar jointing, with individual flows up to 30 m thick (Wilson & Manning 1978). In the south, the period of dormancy was interrupted by emplacement of the massive Tardree rhyolite of the IBF (Old 1975). The rhyolite represents the final differentiates of the first volcanic cycle (Lyle 1980). Around 30 dolerite plugs and numerous dykes cut the ALG and are presumed to have functioned as feeders for higher level flows. Their orientation follows the main dyke trend that is NNW–SSE (Walker 1959). The ALG lies in an open syncline with axis trending NNW–SSE parallel to the main dyke trend. Flow dips rarely exceed 10°. In the proximity of the hinge line east of Lough Neagh (Fig. 1c), the Langford Lodge borehole has documented the thickness of the LBF to be 531 m (Manning *et al.* 1960). The UBF has a documented thickness of 346 m in the BallyMcillroy no. 1 borehole north of Lough Neagh (Fig. 1c: Thompson 1979). Both formations thin towards the present day margins of the depression.

Geochronology

In the present contribution we have recalculated all $^{40}Ar/^{39}Ar$ ages from the literature to conform with the recommended fluence monitor ages (Renne *et al.* 1998). All ages adjusted by us are marked with the subscript *R*. In Fig. 2, numbers associated with a date are numbered according to the text appearing later, while numbers inside circles are paleomagnetic sampling sites. Ages are reported at the 1σ level unless otherwise stated.

Reliable ages have been published for much of the pre-drift lava succession of the NAIP. However, the chronology of emplacement of the ALG is often left unmentioned in the literature. A study by Thompson (1985), using the $^{40}Ar/^{39}Ar$ method, left the age of the LBF inconclusive, but a date of 61.6 ± 0.6 Ma_R was obtained for the Tardree rhyolite (IBF; 1 in Fig. 2a), and 58.9 ± 1.1 Ma_R for the UBF (2 in Fig. 2a). Meighan *et al.* (1988) reported a Rb/Sr date of 60.3 ± 1.4 Ma for the Tardree rhyolite (IBF; 3 in Fig. 2a). Thompson's (1985) and Meighan *et al.*'s (1988) dates for the Tardree rhyolite are compatible with Gould's (2004) U-Pb date of 60.9 ± 0.5 Ma (4 in Fig. 2a) for detrital zircons from a laterite layer underlying the Causeway Tholeiites (IBF) in the north (the zircons that are thought to have Tardree as a source). However, Gamble *et al.* (1999) reported a younger date for the Tardree rhyolite of 58.4 ± 0.7 Ma (5 in Fig. 2a) using the U-Pb SHRIMP method.

An $^{40}Ar/^{39}Ar$ study by Chambers (2000) dated samples from all three Formations of the ALG: (1) $\sim$62 Ma_R was obtained for the LBF (6–9 in Fig. 2a); (2) 61.1 ± 0.3 Ma_R was obtained for several sanidine samples from the Sandy Braes obsidian (IBF; 10 in Fig. 2a); (3) a total gas age of 62.1 ± 0.4 Ma_R gives a maximum age for the Causeway Tholeiites (IBF), but suffers from recoil effects

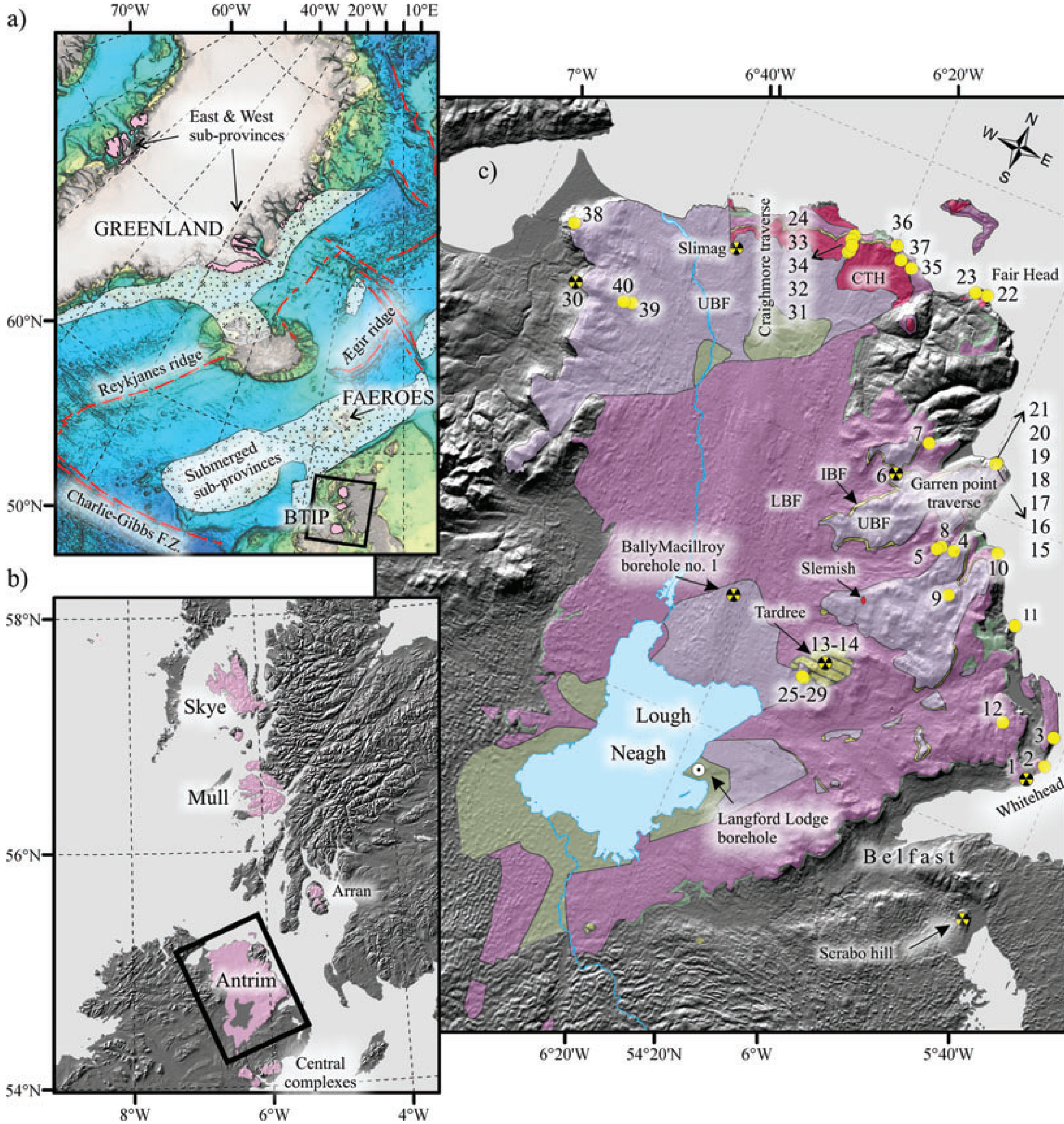

Figure 1. (a) The geologic outline of the North Atlantic Igneous Province, (b) the British Tertiary Igneous Province and (c) the Antrim Lava Group. Yellow (yellow and black) circles are paleomagnetic (and/or $^{40}Ar/^{39}Ar$ analysis) sampling sites. Submerged subprovinces are from Larsen & Saunders (1998). The BallyMacillroy no. 1 and Langford Lodge boreholes are shown north and east of Lough Neagh. LBF, IBF and UBF denote Lower, Inter and Upper Basalt Formation, while CHT denotes Causeway Tholeiite member.

and excess argon, and is inconsistent with the younger age of the stratigraphically lower LBF, and (4) a pseudo plateau age of 59.7 ± 0.4 Ma_R was obtained for the UBF (11 in Fig. 2a).

Paleomagnetism

The paleomagnetic investigation is also part of a larger programme led by us to produce new paleomagnetic poles for the lava sequences of the BTIP (Ganerød *et al.* 2008). Recent and very welcome studies have been performed on the extensive lava sequences in Western Greenland by Riisager & Abrahamsen (1999), Riisager *et al.* (2003a) and Riisager *et al.* (2003b) and the Faeroe Islands lavas by Riisager *et al.* (2002). The lava sequences of the BTIP on the other hand, have not received much attention paleomagnetically since the 1970s (Wilson 1970; Løvlie *et al.* 1972; Hall *et al.* 1977; Mussett *et al.* 1980). Following their work in Western Greenland (Riisager *et al.* 2003a; Riisager *et al.* 2003b) and the Faeroes Islands (Riisager *et al.* 2002), Riisager *et al.* (2003b) noted similarity

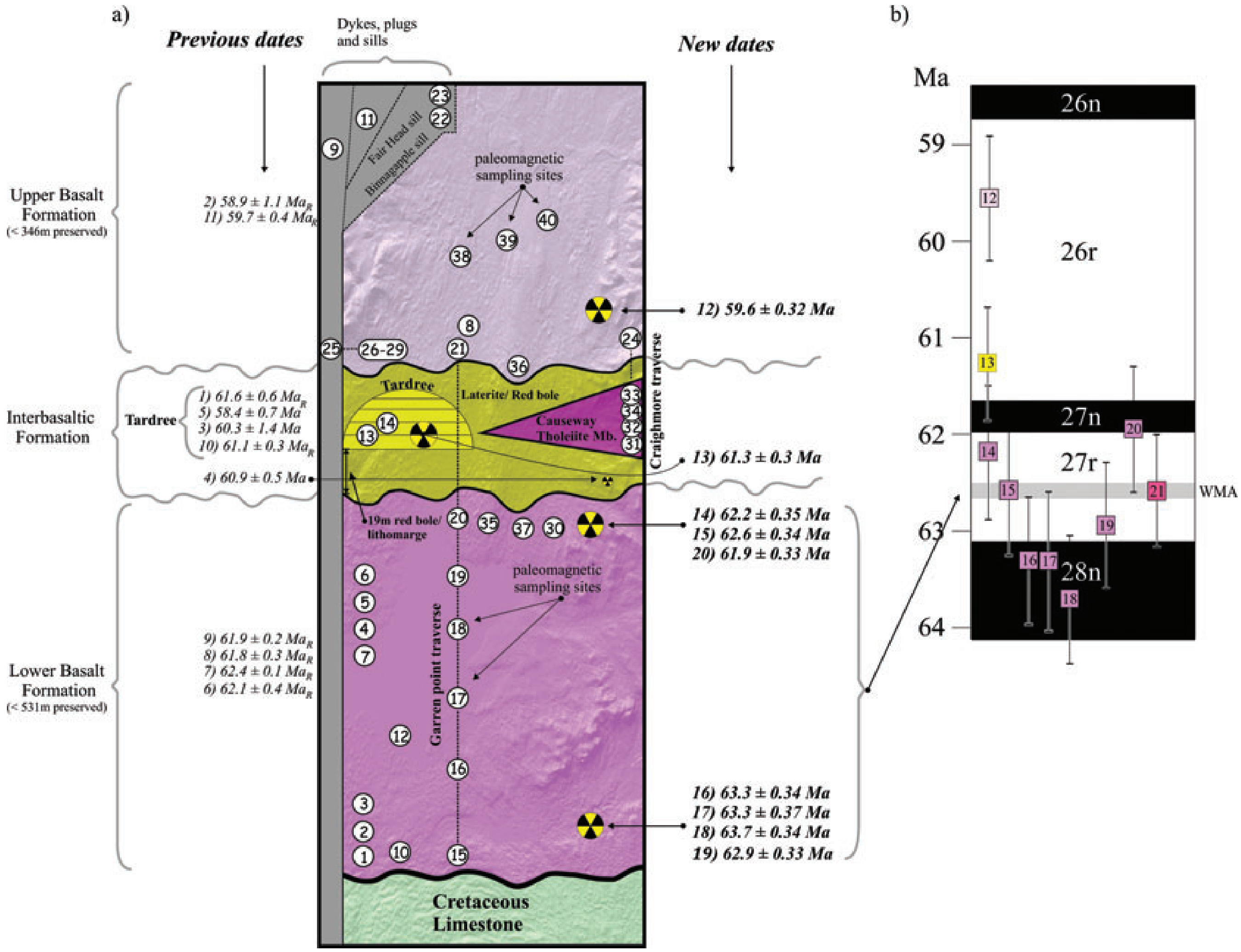

Figure 2. (a) The stratigraphy of the Antrim Lava Group. The ALG consists of the Lower Basalt, Interbasaltic and the Upper Basalt Formations. The Tardree Rhyolite Complex and the Causeway Tholeiite Members are situated in the Interbasaltic Fm. Numbered white circles show the locations of the paleomagnetic sampling sites and the paleomagnetic remanence polarities observed at the sites (white = reverse). Sites on two paleomagnetic sampling traverses are shown with connecting lines. Previous age determinations are shown on the left of the column, whereas the new ages obtained by us are shown on the right, with approximate locations shown by yellow and black circles. Subscript *R* means recalculated ages. The references for the dates in (a) are: (1, 2): Thompson (1985) shown recalculated (17.19 → 17.37 Ma for the B4b monitor), (3) Meighan *et al.* (1988), (4) Gould (2004), (5): Gamble *et al.* (1999), (6–11) Chambers (2000) shown recalculated (27.92 → 28.34 Ma for the TCR monitor) and (12–19) this study. (b) The new dates are shown with 95 per cent confidence limits in relation to the geomagnetic polarity timescale of Ogg & Smith (2004).

between the paleomagnetic poles from these two subprovinces after correcting for the later opening of the North Atlantic. However, Riisager *et al.* (2002) reported that the British paleomagnetic data differed significantly from their Faeroes result, even though both subprovinces reside on the same plate. They suggested that the predominantly old paleomagnetic studies in the BTIP are less reliable and attributed the discordance to this.

Ganerød *et al.* (2008) reexamined the magnetic signature in the Isle of Mull lavas and were able to verify the earlier results of Hall *et al.* (1977). Furthermore, their reexamination of all paleomagnetic data from the NAIP indicated that the differences that concerned Riisager *et al.* (2002) are not significant and suggested that there are curious differences between some of the paleomagnetic data within the western Greenland domain. Further on this issue, we are able to report that a reinvestigation of the Skye Lavas by Rousse *et al.* (in preparation) has produced a paleomagnetic pole consistent with the recent Mull result of Ganerød *et al.* (2008). To conclude our initiative to reexamine the paleomagnetic histories of the lava sequences of the BTIP, we present a new paleomagnetic pole for the last of the expansive lava fields; the Antrim Lavas of Northern Ireland. Apart from anisotropy of a magnetic susceptibility flow pattern study of Gould (2004), this contribution is the first paleomagnetic study of the ALG since Løvlie *et al.* (1972).

SAMPLING

Sampling for paleomagnetic analysis focused on the east and the north coast of Antrim where fresh outcrops and continuous stratigraphic sections through the lava sequences are accessible. A total of 349 25-mm-diameter drill cores were extracted at 40 sites (Figs 1c and 2a, Table 2). Special effort was made to achieve a horizontal and vertical spread in sampling sites to examine the effects of tilting across the syncline and to obtain stratigraphic control on the paleomagnetic record. Two detailed sampling traverses were carried out; one at Garren Point through the LBF up to the first flow in the UBF (sites 15–21), and a second through the CM ending at the first flow in the UBF on the hilltop of Craighmore (sites 31, 32, 34, 33, 24). Two paleomagnetic sampling sites were established in a quarry in the Tardree rhyolite (sites 13 and 14). Four intrusive units were sampled; two dolerite plugs (sites 9 and 11) and two sills at Fair Head—the Binnagapple sill (lowermost, site 22) and Fair Head sill (uppermost, site 23). We assume that the intrusives are time equivalent to the lavas, also shown by a recent 60.2 ± 0.4 Ma age determination for the Fair Head sill (McKenna *et al.* 2009).

Additional material was collected at the paleomagnetic sampling sites for $^{40}Ar/^{39}Ar$ dating, however much of this material proved unsuitable for dating. Sampling sites for $^{40}Ar/^{39}Ar$ analysis are marked as yellow and black circles in Fig. 1. The Geological Survey of Northern Ireland very kindly gave us permission to sample rock extracted from the BallyMcillroy borehole no. 1 north of Lough Neagh (Fig. 1c). The borehole passes through the volcanics where they are thickest (769 m), giving us the opportunity to date the deepest part of the lava pile near the centre of the syncline/depression. In addition, a sample from the Scrabo Hill sill was collected and analysed (Fig. 1c).

RADIOMETRIC DATING

Mineral separation and irradiation

Samples were crushed and sieved to isolate grains of 180–250 μm. Some of this material was set aside for whole rock analysis whereas feldspar grains were selectively extracted from the rest using magnetic and heavy liquid techniques. Conventional mineral separation techniques were then employed (magnetic separation using a Frantz isodynamic magnetic mineral separator followed by heavy liquid separation with lithium polytungstate to separate feldspar from quartz). The whole rock samples were washed in 5M HNO_3 for 5 min to remove carbonate. The mineral separates were washed in acetone several times and finally fresh inclusion-free feldspar grains were handpicked under the binocular microscope. The whole rock and feldspar samples were packed in aluminium capsules together with the Taylor Creek rhyolite (TC) flux monitor standard (between each fifth sample, every ~8 mm) and zero aged K_2SO_4 and CaF_2, and the transformation $^{39}K(n, p)^{39}Ar$ was performed during irradiation at the McMaster nuclear facility. We used the age of 28.34 ± 0.16 Ma for the TC monitor (Renne *et al*. 1998). The correction factors for the production of isotopes from Ca and K can be found in Table S1 (Supporting Information). The feldspar and whole rock samples were step heated in the fully automated $^{40}Ar/^{39}Ar$ lab at the Geological Survey of Norway using either a defocused Merchantek CO_2 laser or a resistance furnace (Heine type). The extracted gases were gathered for first 2 min, then 9 min in a separate part of the extraction line and analysed with an MAP 215–50 mass spectrometer. The peaks were determined during peak hopping (least eight cycles) on the different masses ($^{41-35}Ar$) on a Balzers electron multiplier. Subtraction for blanks, correction for mass fractionation, corrections for ^{37}Ar and ^{39}Ar decay and neutron-induced interference reactions produced in the reactor were done using in-house software (T.H. Torsvik & A.O. Arnaud) that implements the equations in McDougall & Harrison (1999) and the recommended decay constants of Steiger & Jäger (1977). The isotope ^{40}Ar is assumed to be radiogenic and atmospheric (after correction for the blank and neutron induced interference reactions) and all ^{36}Ar to be atmospheric; therefore, a $^{40}Ar/^{36}A$ ratio of 295.5 (Nier 1950) is used in each calculation step. In choosing the steps we followed the recommendation of McDougall & Harrison (1999). We calculated weighted mean plateau ages (WMPA, weighting on variance and percentage of ^{39}Ar) where each step overlapped at the 95 per cent confidence level.

$^{40}Ar/^{39}Ar$ results

The age spectra, K/Ca, and the $^{38}Ar_{Cl}/^{39}Ar_K$ ratios for the samples are presented in Figs. 3(a)–(j). The main results of the heating experiments are listed in Table 1, whereas the experimental data for each sample and the inverse isochron diagrams are found in Table S1 and Fig. S1(a)–(j) (Supporting Information). The raw data for the Tardree sample is reported in Ganerød *et al.* (2010) but we include the spectrum and inverse isochron here (Figs 3b and S2b) for completeness of the ALG geochronology.

Valid plateau ages were obtained in all analysis. The corresponding mean square of weighted deviances (MSWD) indicates a good correspondence between the expected and estimated errors (Table 1). Our new analysis reveals an age of 59.6 ± 0.3 Ma for the UBF (12 in Figs 2a and b and 3a); a result statistically indistinguishable from the UBF ages reported by Thompson (1985) and Chambers (2000). Ganerød *et al.* (2010) report an age of 61.3 ± 0.3 Ma (Fig. 3b) for the Tardree rhyolite of the IBF, which corresponds to a U-Pb age of 61.3 ± 0.11 Ma from the same location (13 and 14 in Figs 1c and 2a). The WMPAs of the seven samples analysed by us from the LBF meet the reliable criteria (Figs 2b and 3c–i). Keady Mt. (site 20) is mapped as UBF by the Geological Survey of Northern Ireland (1997), but our age determination leads us to support the LBF interpretation for this location offered by Cooper (2004, p. 171).

We calculate a weighted mean age (WMA) of the WMPAs for the seven LBF samples (Table 2). We exclude the error on J in the WMA, only experimental errors are used for weighting. This gives a WMA of 62.63 ± 0.02 Ma ($n = 7$), which combined with the error on J (0.5 per cent) gives 62.63 ± 0.31 Ma (nr. 21 in Fig. 2b; Table 1).

PALEOMAGNETIC ANALYSIS

Paleomagnetic laboratory experiments were carried out at the Geological Survey of Norway. Natural remanent magnetization (NRM) was measured using AGICO JR6A spinner magnetometers, mounted within a Helmholtz coil system. Components of magnetization were identified using stepwise thermal demagnetization. In total, 349 specimens were thermally demagnetised using 15–25 heating steps. The directions and unblocking temperature spectra of characteristic remanence components (ChRM) were determined using the LineFind algorithm of Kent *et al.* (1983) as implemented in the Super-IAPD program available at www.geodynamics.no (Torsvik *et al.* 2000).

Basaltic lavas of the LBF, CM and UBF

The majority of the specimens carry a single component of magnetization (Figs 4a–c) carried by grain populations with Curie points at 500, 580 and 680 °C. From this we deduce the carriers to be a mixture of titanium-poor magnetite/titano-magnetite and hematite/titano-hematite. All the characteristic component directions obtained from the basaltic lavas of the LBF, CM and UBF are of reverse polarity (Table 2). Hospers & Charlesworth (1954), Wilson (1970) and Løvlie *et al.* (1972) also observed reverse polarity remanence at their sampling sites in these lava sequences.

We performed a baked contact test for the stability of paleomagnetic remanence spanning sites 25, 26 and 27 where a 5.5-m-wide dyke penetrates the UBF (Table 2). The dyke and host lava flow both carry reverse polarity remanence, but their oblique alignment

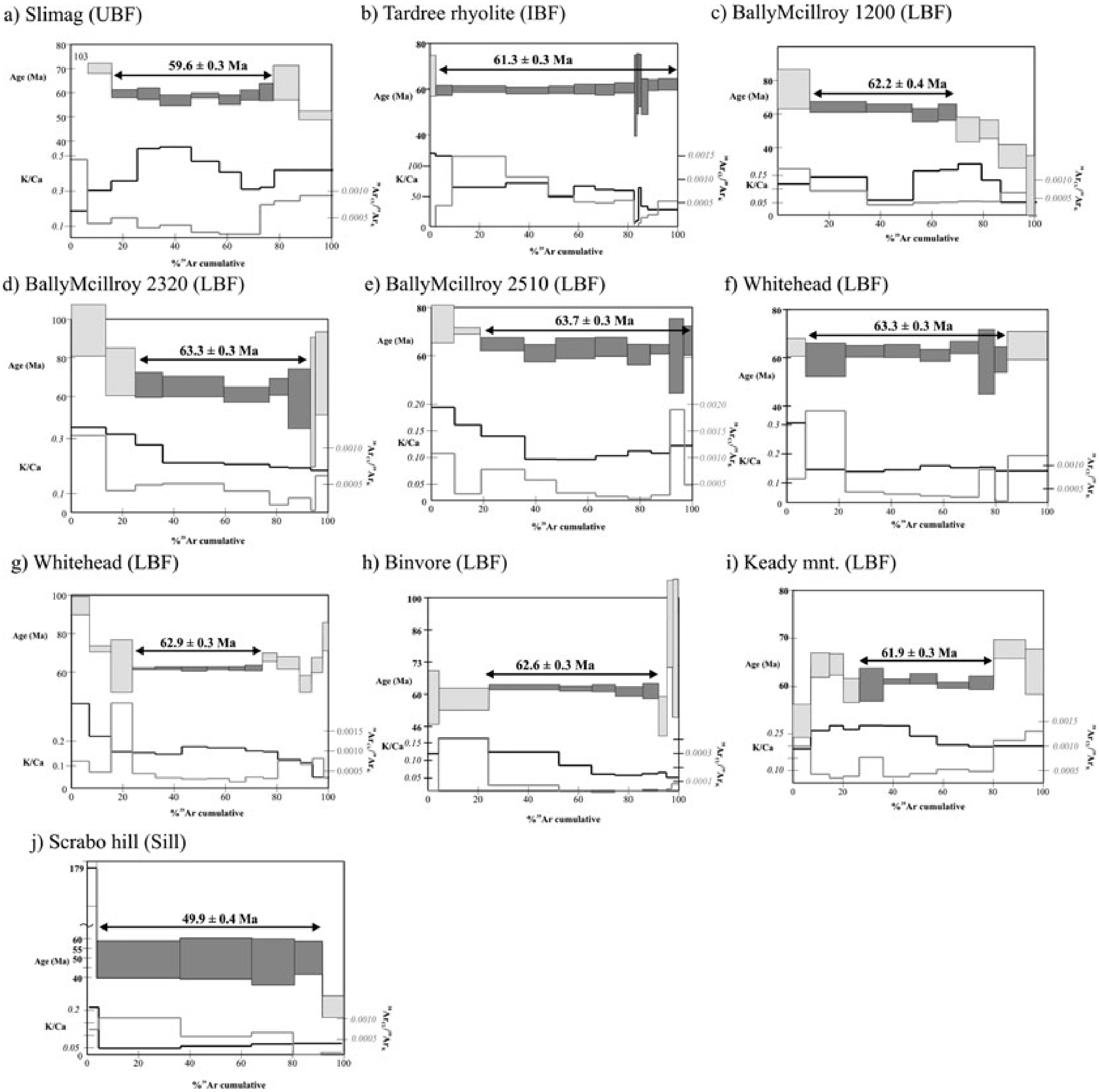

Figure 3. Results of $^{40}Ar/^{39}Ar$ analysis. The error bars are at the 2σ level without the experimental error on the J-value. The ages obtained on the plateaus are weighted on the inverse of the variance and length (percentage of ^{39}Ar). The K/Ca ($^{38}Ar_{Cl}/^{39}Ar_K$) ratios are show by the black (grey) lines under the plateaus.

permits recognition of the dyke direction in the country rock near the dyke, giving way to the lava flow direction away from the dyke. We do not observe both directions together in a single specimen so we treat this test as a partial positive contact test. This and the magnetic properties of the material indicate a primary or near primary origin for the characteristic remanence in the lava sequence. The magnetic polarity determinations obtained from the lava sites are stratigraphically linked to the radiometric age determinations in Fig. 2.

Tardree rhyolite

The remarkable phenomenon of self-reversal of magnetic remanence is observed at sampling site 14 in the rhyolite (Fig. 4e). A normal polarity component with low stability unblocks up to treatments of 200 °C, presumed to be a record of the recent magnetic field. Then reversed, normal and finally reversed magnetizations are removed up to treatments of 680 °C (Fig. 4e). The magnetization alignment is the same at the characteristic remanence in the lava sequence.

Intrusives

Samples from the plugs, dykes and sills exhibit magnetic characteristics similar to those of the lava sequence (Fig. 4d); the directions of magnetization are indiscernible from those carried by the lavas sequence, and all show reversed polarity.

Table 1. Main $^{40}Ar/^{39}Ar$ results from heating experiments.

F	Comment	Name	Spectrum analysis					Inverse isochron analysis		
			^{39}Ar (per cent)	Steps	Age (Ma) ± 1σ (wJ)	1σ (woJ)	MSWD	Age (Ma) ± 1σ	MSWD	Intercept ±1σ
UBF	L,W,12,NA	Slimag	61.9	3–9	59.6 ± 0.32	0.052	1.31	59.65 ± 0.55	1.03	296 ± 0.4
IBF	I,K,13,13	Tardree rhyolite	97.7	2–14	61.3 ± 0.3	0.05	0.7	61.1 ± 0.5	0.46	298.6 ± 5.8
LBF	U,W,14,NA	BallyMcillroy 1200	57.1	2–5	62.2 ± 0.35*	0.143	1.29	63.35 ± 2.02	1.42	294.7 ± 1.8
LBF	M,W,17,NA	BallyMcillroy 2320	68.3	3–7	63.3 ± 0.37*	0.157	0.88	62.38 ± 2.16	0.79	299 ± 4.6
LBF	L,W,18,NA	BallyMcillroy 2510	81.1	3–10	63.7 ± 0.34*	0.08	0.76	64.1 ± 0.8	0.75	295.6 ± 0.5
LBF	L,W,16,1	Whitehead 2	77.3	2–8	63.3 ± 0.34*	0.09	1.06	63.94 ± 0.75	0.78	294.6 ± 0.77
LBF	L,W,19,1	Whitehead 3	50.7	4–9	62.92 ± 0.33*	0.025	0.24	63.3 ± 0.36	0.16	295 ± 0.9
LBF	U,W,15,6	Binvore	67.7	3–7	62.6 ± 0.34*	0.044	0.96	63.2 ± 0.6	0.86	294.8 ± 2.1
LBF	L,W,20,30	Keady Mt	59.9	4–9	61.9 ± 0.33*	0.032	1.02	62.5 ± 0.46	0.74	293.9 ± 1.5
Sill	I,P,NA,NA	Scrabo hill	87.8	2–5	49.9 ± 0.43	0.362	0.03	49.6 ± 1.08	0.04	296.1 ± 6.1
LBF	NA,NA,21,NA	Weighted mean age of LBF			62.63 ± 0.31	0.002				

Note: The age of 28.34 Ma is used for the USGS TC sanidine monitor (85G003) in the original data reductions. F denotes formation. The symbols in the comment column are as follows: approximate position in the formation (L, lower; M, middle; U, upper; I, intrusive), type of material (W, whole rock; P, plagioclase; K, K-feldspar), number in Fig. 2b and paleomagnetic site (NA, not available). The samples in asterisk are used in the weighted mean age for the LBF (bottom). The errors are quoted with (wJ) and without (woJ) the experimental errors on the J.

Paleomagnetic pole

Most of the results come from lava flows of the LBF, CM and UBF. The rest are from intrusive rocks (three sites: 11, 22 and 23) close in age to the UBF. Field relationships between our sampling sites show that site-level results are likely to represent separate spot readings of the geomagnetic field. Given that successive lava flows can be emplaced over a short time interval, adjacent flows may record the same spot value of the field. To reduce the probability of this happening in our data set, we sampled at wide stratigraphic intervals. Although noted by Wilson (1970) in his sampling programme, we see no compelling evidence for this phenomenon in our data set. We assume that the dips (Table 2) in the flows are secondary, post-dating acquisition of the magnetic remanence, and therefore apply a tectonic correction to the site mean directions (Table 2; Fig. 5). All sites contained 5–12 samples. Lava sites should represent spot readings of the Earth's magnetic field, and within-site scatter should be randomly dispersed. Therefore, we applied Fisher (1953) statistics on the directions within a single lava site to calculate site means (Table 2). Because dispersion within a single lava site should be minimal, sites with k-value lower than 50 are normally discarded (see, e.g. Biggin *et al.* 2008; Johnson *et al.* 2008). All our sites provide k-values well above this cut-off. To obtain a time-averaged estimate of the paleofield direction, we take the corrected site mean directions from all 37 sites and calculate the overall mean direction. Averages and cones of confidence were determined using Fisher (1953) statistics applied on virtual geomagnetic poles (VGP), because these are more Fisherian (i.e. a Gaussian dispersed on a sphere) than directions, which have a (latitude dependent) elongated distribution (Tauxe & Kent 2004; Tauxe *et al.* 2008). Errors in declination and inclination are given separately, as ΔD_x and ΔI_x, following Butler (1992). To exclude outliers and transitional directions, we applied the Vandamme (1994) variable cut-off procedure, but no directions were eliminated. The resulting direction is $D \pm \Delta D_x = 181.3^\circ \pm 8.5$ and $I \pm \Delta I_x = -61.3^\circ \pm 5.3$ ($N = 37$, Table 2). The tectonic correction is small and the paleomagnetic fold test performed in Table 2 does not prove the age relation between remanence acquisition and introduction of the flow dips at the 95 per cent confidence level. Application of the dip adjustment only affects the resulting mean direction by 1.3° of arc so a solution to this uncertainty is not essential.

The degree of paleosecular variation (PSV) is usually expressed in terms of the angular standard deviation (ASD) of VGPs with the implicit assumption that the distribution is Fisherian (Fisher 1953). The goodness of fit to the Fisherian distribution for the ALG VGPs is lower than the critical values ($Mu = 1.168 < 1.207$, $Me = 0.464 < 1.094$) and the null hypothesis that the distribution of VGPs is Fisherian cannot be rejected at the 95 per cent confidence level (Fisher *et al.* 1987). The ASD of VGPs, corrected for within flow dispersion $Sw = 4.6^\circ$ (McFadden *et al.* 1991) is 23° with a 95 per cent confidence limit (Cox 1969) of $16.1 \leq ASD \leq 30.8$. This ASD is within error of the PSV prediction of the G-model of McFadden *et al.* (1991), which indicates an ASD value of ~17 for this time and paleolatitude. We therefore conclude that determination of the overall mean direction from tilt-corrected flow results (Fig. 5b) satisfactorily averages out paleosecular variation.

For this data set we calculated an apparent paleomagnetic pole position at 78.9°N, 167.0°E (A95 = 6.3, K = 15.0; star in Fig. 6, Table 3).

DISCUSSION

Continuity of paleomagnetic poles across the NAIP

Ganerød *et al.* (2008) compiled and evaluated paleomagnetic results from the peer-reviewed literature and compared their new pole for the Isle of Mull to the rest of BTIP and NAIP, and concluded that their pole overlaps with most of the other studies from the province. We use the pole collection of Ganerød *et al.* (2008) with some modifications (Table 3); the newer pole from the Isle of Mull supersedes that of Hall *et al.* (1977) and Ade-Hall *et al.* (1972), and we include a new unpublished pole from the Isle of Skye (Rousse *et al.* in preparation). For comparison with the rest of the NAIP we use the mean poles from East and West Greenland of Ganerød *et al.* (2008). Poles are shown in Fig. 6; results from the BTIP are shown with black circles and the new ALG pole is labelled 'An.' The new poles from Mull and Skye are labelled 'M' and 'S', respectively. All other poles are labelled as in Table 3. Our new pole from the ALG is consistent with earlier studies form the same lava formations in Northern Ireland (Wilson 1970; Løvlie *et al.* 1972). Furthermore, the new ALG result resembles the recent Mull and Skye poles,

Table 2. Paleomagnetic sampling sites and results.

Site	Unit	Comment	sLat	sLong	*D*	*I*	Strike	Dip	D_{str}	I_{str}	*N*/*n*	*k*	a_{95}	VGP_{lat}	VGP_{long}	NRM_{int}	Sus	Polarity
1	LBF*	Whitehead	54.747	−5.712	169.2	−58.4	245	21	164.4	−37.8	10/10	118.3	4.5	54.4	199.8	0.25	970	R
2	LBF*		54.768	−5.689	202.1	−53.4	335	15	212.2	−41.5	6/6	590.5	1.6	51	123.6	0.67	1632	R
3	LBF*		54.801	−5.695	175.6	−45.5	140	5	171.1	−48.3	11/11	157.2	3.0	63.7	192	3.53	5271	R
4	LBF*		54.947	−6.031	162.0	−63.9	0	0	162.0	−63.9	11/11	134.5	4.6	75.2	232.1	13.67	18767	R
5a	LBF*	Two flows	54.943	−6.037	192.7	−68.3	0	0	192.7	−68.3	6/6	504.2	2.5	81.7	103.2	21.63	22161	R
5b	LBF*				175.2	−65.7	0	0	175.2	−65.7	6/6	246	3.3	82.4	198.9	5.74	15373	R
6	LBF*		55.002	−6.164	176.7	−62.3	154	19	138.5	−63.6	6/7	212	3.8	62.1	260.7	1.08	3759	R
7	LBF*		55.047	−6.128	213.0	−61.4	0	0	213.0	−61.4	6/8	332.6	3.0	65.3	100.3	0.88	3168	R
8	UBF*		54.949	−6.005	181.9	−61.0	160	10	163.3	−63.2	9/9	99.9	3.5	75.2	227.1	4.2	8142	R
9	UBF*		55.904	−5.985	159.4	−37.6	0	0	159.1	−37.6	9/9	258.8	3.2	51.8	206.6	1.5	10583	R
10	LBF*		54.964	−5.926	160.3	−51.9	130	10	147.7	−56.0	12/12	154.9	3.1	60.9	236	0.59	5114	R
11	Plug*		54.898	−5.843	176.0	−62.7	0	0	176.0	−62.7	9/9	176.7	3.1	78.9	189.2	2.97	17121	R
12	LBF*		54.795	−5.795	215.4	−72.6	0	0	215.4	−72.6	9/10	154.8	3.7	70.4	60.5	0.76	3264	R
13	IBF*	TRC	54.781	−6.149	208.8	−55.4	0	0	208.8	−55.4	13/17	61.7	4.6	62.7	115.6	0.17	8343	R/N
14	IBF						0	0								0.08	7507	R/N
15	LBF*	Gpt 1	55.056	−5.994	218.0	−55.4	117	5	219.6	−60.3	5/5	170.7	5.9	60.7	95.5	0.71	1342	R
16	LBF*	Gpt 2	55.056	−5.994	181.0	−57.3	117	5	177.0	−61.7	8/11	549.9	2.9	77.7	184.4	2.13	9215	R
17*	LBF*	Gpt 3	55.056	−5.994	188.6	−64.9	117	5	184.4	−69.6	9/9	238.1	3.3	86.9	115.6	1.47	8600	R
18*	LBF*	Gpt 4	55.056	−5.994	211.2	−64.6	117	5	212.2	−69.6	7/7	114.9	4.3	71.3	75.8	1.79	19146	R
19*	LBF*	Gpt 5	55.056	−5.994	176.4	−53.5	117	5	172.5	−57.7	6/7	126.2	4.6	72.5	194	2.26	17715	R
20*	LBF*	Gpt 6	55.056	−5.994	178.9	−42.3	117	3	177.5	−44.9	7/8	70.3	7.2	61.4	178.7	1.46	27695	R
21*	UBF*	Gpt 7	55.054	−5.995	149.3	−43.5	117	0	149.3	−43.5	7/8	160.5	3.6	52.8	223.7	2.33	15183	R
22*	Sill*	Binnagapple sill	55.221	−6.134	168.1	−64.9	0	0	168.1	−64.9	7/8	185.9	4.9	78.8	220.5	1.88	18162	R
23*	Sill*	Fair Head sill	55.220	−6.157	161.9	−54.7	0	0	161.9	−54.7	10/10	51.2	6.8	66.4	213.3	2.0	17273	R
24	UBF*	Craigh 5	55.207	−6.413	196.2	−58.8	0	0	196.2	−58.8	5/8	244	4.9	71	132.3	3.85	3136	R

Table 2. (*Continued.*)

Site	Unit	Comment	sLat	sLong	D	I	Strike	Dip	D_{str}	I_{str}	N/n	k	α_{95}	VGP_{lat}	VGP_{long}	NRM_{int}	Sus	Polarity
25	Dyke*	Ct	54.757	−6.176	166.3	−49.6	30	10	176.6	−55.9	11/12	264.8	2.3	71.5	182.5	4.16	14163	R
26	UBF**	Ct	54.757	−6.176	–	–	–	–	–	–	0/11	–	–			5.3	9688	R
27	UBF	Ct	54.757	−6.179	183.5	−72.2	30	10	216.5	−74.0	5/6	477.3	2.8	69.9	53.4	26.41	34069	R
28	UBF	Ct	54.757	−6.178	175.7	−75.9	30	10	219.4	−78.2	6/7	592.3	3.8	67.7	34.1	3.97	12398	R
29	UBF	Ct	54.758	−6.180	172.3	−78.4	30	10	227.1	−80.4	8/8	189.6	3.5	64.1	26.3	2.37	7265	R
	UBF*	27,28,29 comb	54.757	−6.180	170.6	−76.1	30	10	215.7	−79.2	19/21	184.9	2.3	68.5	28.3	–	–	–
30	LBF*	Keady mnt.	55.059	−6.871	203.3	−52.4	355	10	213.2	−46.9	6/9	53.8	8.3	54	117.9	1.44	8305	R
31	IBF*	Craigh 1	55.226	−6.413	166.5	−64.2	90	3	164.9	−67.1	7/7	632.7	2.4	79.4	239.2	4.57	6376	R
32	IBF*	Craigh 2	55.221	−6.415	156.4	−46.6	90	3	155.0	−49.3	7/7	367	3.5	59.3	219.3	0.98	8970	R
33	IBF*	Craigh 4	55.209	−6.410	189.0	−72.0	90	3	190.7	−75.0	5/8	3227.1	1.6	81.4	29.4	4.58	7049	R
34	IBF*	Craigh 3	55.215	−6.410	190.2	−64.9	90	3	191.5	−67.8	8/8	71.8	5.7	81.8	111.5	0.92	8460	R
35	IBF*		55.217	−6.289	218.9	−46.3	0	0	218.9	−46.3	6/7	340.2	3.3	50.7	112.2	1.27	11656	R
36	LBF*		55.221	−6.313	172.1	−48.8	240	4	170.5	−45.1	9/10	258.9	3.2	60.6	191.2	3.5	5936	R
37	UBF*		55.234	−6.331	218.9	−60.4	0	0	218.9	−60.4	8/8	155.2	5.4	61.1	96	1.22	5707	R
38	UBF*		55.118	−6.918	192.8	−70.6	0	0	192.8	−70.6	7/8	251.3	3.8	82.7	80	0.72	1460	R
39	UBF*		55.062	−6.756	178.7	−70.4	0	0	178.7	−70.4	8/8	223.8	3.2	89.1	229.1	2.93	2989	R
40	UBF*		55.060	−6.771	166.7	−73.5	0	0	166.7	−73.5	7/8	189.3	3.3	81.6	299.5	1.29	2292	R
Mean for ALG in situ			–	–	182.3	−60.4			–	–	37	33.1	4.2					
Mean for ALG corrected			–	–					181.3	−61.3	37	25.6	4.7	78.9	167	$K = 15.0$	A95 = 6.3	$\Delta D/I = 8.5/5.3$
Mean UBF			–	–					176.7	−65.9	7	26.5	12.0					
Mean IB			–	–					181.3	−60.5	6	19.6	15.5					
Mean LBF			–	–					186.3	−60.8	19	23.9	7.2					
Intrusives (9, 11, 22, 23, 25)			–	–					173.9	−56.4	6	33.2	11.8					

Note. The symbols in the Comment column are as follows: TRC, Tardree Rhyolite Complex; Gpt, Garren point traverse; Craigh, Craighmore traverse; Ct, contact test; sLat/sLong, coordinates of sampling sites (datum WGS84); D/I, declination/inclination of flow mean remanence directions; Strike/Dip, strike and dip of units (right hand rule); D_{str}/I_{str}, tilt corrected directions; N/n, number of remanence directions/specimens; R, length of resultant vector; k and α_{95} are the Fisher (1953) precision parameter and half angle of the cone of 95 per cent confidence. VGP are the coordinates of the virtual geomagnetic poles. NRM_{INT} denotes NRM intensities (A m^{-1}) and Sus are the susceptibilities (10^{-5} SI) before heating. Volumes of specimens are ~11.15 cm^3. Lava flow results marked with an asterisk (*) are used in calculation of the overall mean direction at the bottom of the table while (**) is a baked zone and not used.

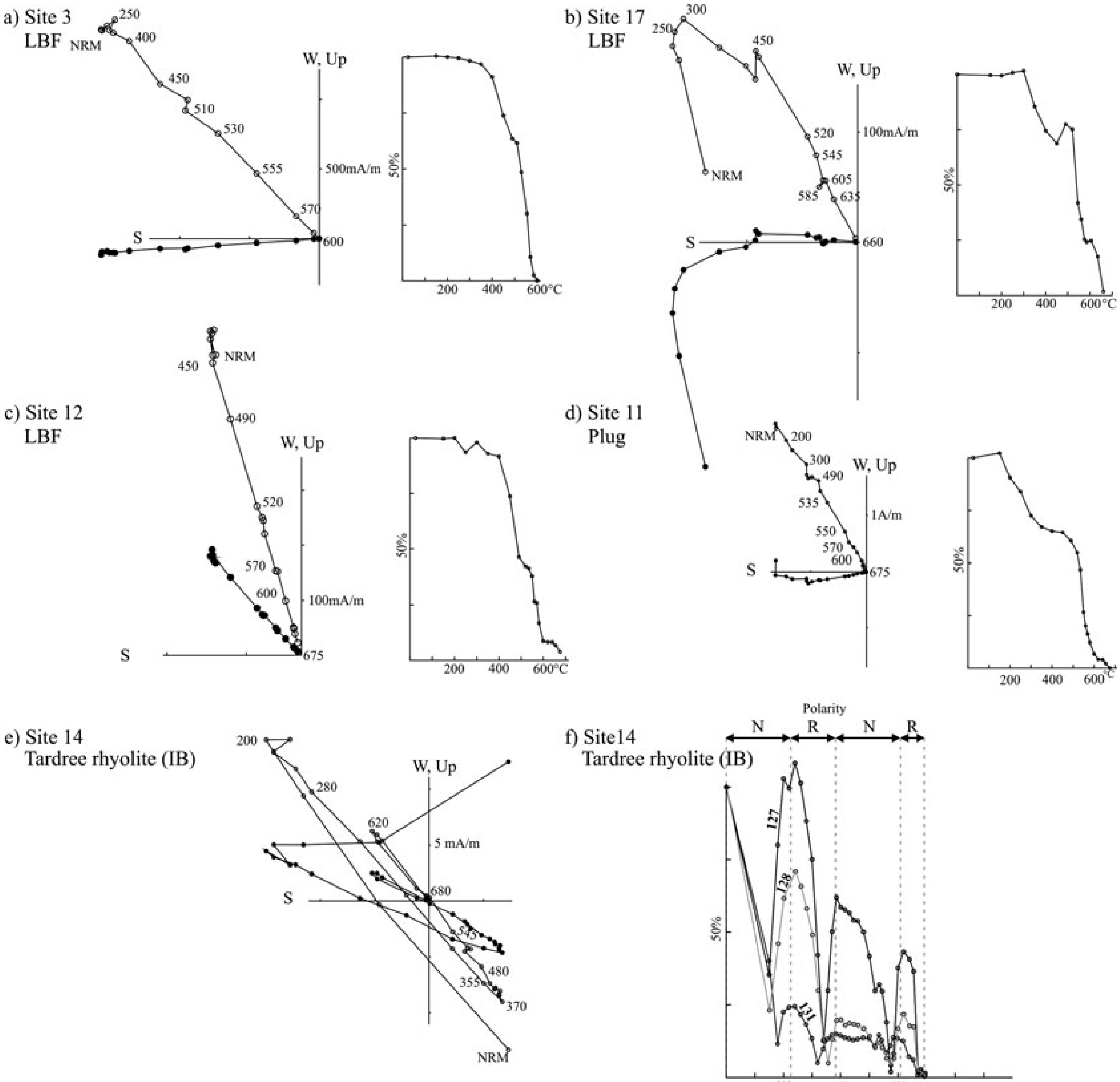

Figure 4. Orthogonal plots, J/J_0 demagnetization curves of stepwise demagnetization data and equal area projection of mean directions for the Antrim Lava Group and intrusives (see also Table 2). Orthogonal plots; solid (open) symbols represent data projected into the horizontal (vertical) plane, (a) typical behaviour of the ALG formation, (b) sample with a normal polarity overprint, (c) single vector component where hematite/titano-hematite is present, (d) saddle-shaped demagnetization spectrum with mixed Curie temperature distributions, (e) orthogonal plot illustrating self-reversal behaviour in a Tardree rhyolite sample, (f) J/J_0 plot for the sample in (e) together with plots for two other samples showing similar unblocking temperature spectra. N and R (above f) indicate the temperature dependent polarities hosted by the mineralogy

results from the rest of the BTIP and Faeroes, and the mean poles for West and East Greenland. We therefore maintain that all of the BTIP lavas record similar pole positions to each other and the rest of the NAIP.

Timing of emplacement of the ALG with respect to the rest of the NAIP

In this study, we present several new $^{40}Ar/^{39}Ar$ dates for the three formations of the ALG, which indicate initiation of eruption of the LBF at 62.63 ± 0.31 Ma (Table 1). We note that Thompson (1985) obtained several old dates for intrusives from west-central Ireland (Blind rock dyke 61.7 ± 0.5 Ma; Killala bay 61.6 ± 0.9 Ma; Doon Hill 62.3 ± 0.7 Ma; Glenlaur gabbro 62.9 ± 2.1 Ma; Droimchogaidh sill 62 ± 0.6 Ma) with a WMA of 61.97 ± 0.18[1] Ma (approximate locations shown in Fig. 7). In deriving these ages Thompson (1985)

[1] Experimental errors not reported, therefore we used a WMA including the error on *J*.

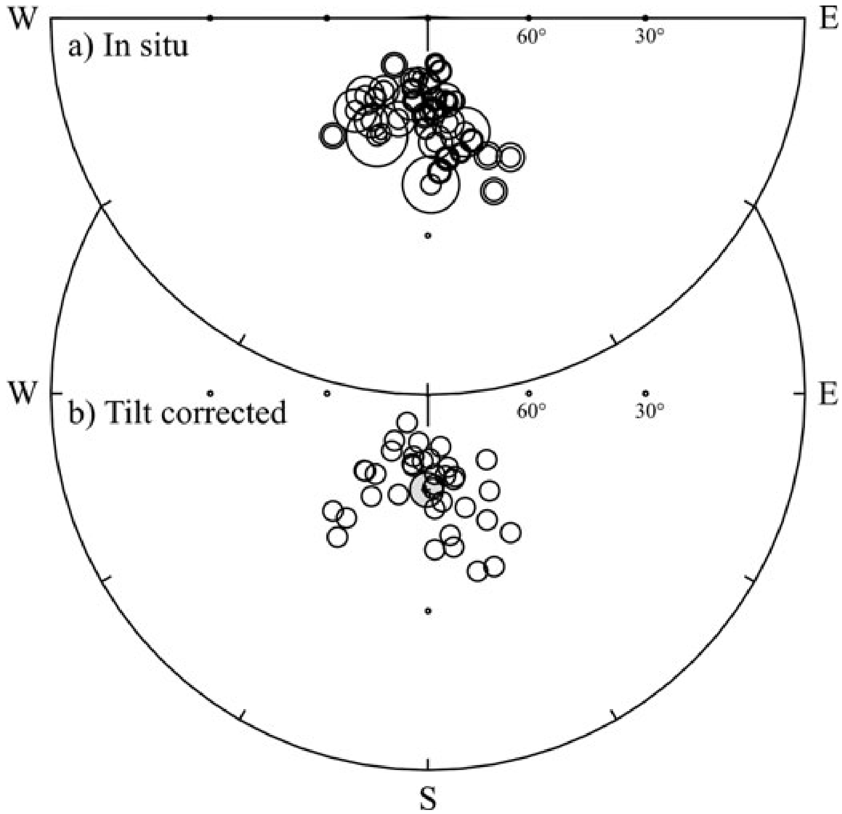

Figure 5. (a) *In situ* directions for 37 units and α95 confidence limits are shown. (b) Tilt corrected mean directions where the overall mean direction is shaded. Equal area projection; open symbols are projected onto the upper hemisphere.

used an age of 17.19 Ma for the B4 biotite fluence monitor. Adopting Baksi *et al.*'s (1996), 17.37 Ma age for the same monitor (intercalibrated with an age of 28.34 Ma for the TC monitor) the weighed mean age for the intrusions becomes 62.6 ± 0.18 Ma_R, close to the age of the LBF from this study. We suspect then, that these bodies may be feeder systems related to lateral equivalents of the LBF, now removed by erosion.

Ganerød *et al.* (2010) combined U-Pb and $^{40}Ar/^{39}Ar$ geochronology on the Tardree rhyolite and obtained a close resemblance between the two methods. The high precision U-Pb age of 61.31 ± 0.11 Ma (2σ) was interpreted as the best age estimate for these rhyolites. The Tardree rhyolite represents a very important time stratigraphic unit in the ALG because it contains high-quality potassium feldspars and zircons so that a reliable date from this unit will fix the IBF in its right time window relative to the LBF and UBF. Furthermore, these rhyolites overlie at least 19 m of laterites of the LBF (Old 1975). Lateritization of basalts are a time-consuming process (Pillans 1997; Hill *et al.* 2000) giving further constraints on the age of the LBF.

The sample from the UBF gave a date of 59.6 ± 0.3 Ma and is statistically indistinguishable from the dates reported by Chambers (2000) and Thompson (1985). We also report a 49.9 ± 0.4 Ma date for the sill at Scrabo Hill. Episodic magmatism has been proposed elsewhere in the NAIP (White & Lovell 1997) and we note three distinct phases in Antrim: ~62.6, ~59.6 and ~50 Ma. These events coincide approximately with ages from drill samples from southeast Greenland (Sinton and Duncan 1998; Tegner & Duncan 1999a) and seamounts in the Rockall through (O'Connor *et al.* 2000).

The dates obtained from the lower part and the upper part of the LBF in the BallyMcillroy borehole can be distinguished at the 95 per cent confidence level (Figs 3c–e; Table 1). This difference is echoed in samples from the LBF elsewhere in Antrim (Table 1); however, we are reluctant to use this difference to infer a duration for emplacement of the LBF. We estimate the total time taken to form the whole ALG to be 3 ± 0.63 Ma (the difference between the WMAs for the LBF and the UBF). This duration is comparable to that proposed for the lava sequence on the Isle of Mull by Chambers & Pringle (2001).

The aforementioned dates for LBF, IBF and UBF can be used as a measure of the lateritization process of the LBF (IBF in Fig. 1). Nineteen metres thickness of laterite between the LBF and Tardree has been documented (Old 1975), and a maximum of 30 m between the LBF and UBF (Hill *et al.* 2000). If we assume rapid emplacement of the LBF and UBF, and a constant process, the weathering gradient was 14.3 mMa^{-1} ($9.8_{min}/26.4_{max}$) between the LBF and Tardree (using 1.3 ± 0.61 Ma), whereas a more precise constraint can be obtained between the LBF and UBF, which gives a weathering gradient of 9.9 mMa^{-1} ($8.2_{min}/12.5_{max}$). Both gradients calculated here are above the global average (6 mMa^{-1}, Wakatsuki & Rasyidin 1992) but compatible with other studies (Théveniaut & Freyssinet 1999), although extreme weathering rates have been documented (Pillans 1997; White *et al.* 1998).

The present and all previous paleomagnetic investigations of the ALG (Hospers & Charlesworth 1954; Wilson 1963; Wilson 1970; Løvlie *et al.* 1972) report reverse magnetic polarity remanence throughout the sampled sections. In Fig. 2b, we plot our new polarity fixes alongside our new $^{40}Ar/^{39}Ar$ age determinations. The geomagnetic polarity timescale of Ogg & Smith (2004) is shown on the right side of the figure. The radiometric ages span chrons C26r, C27n and C27r, placing the LBF in C27r and the UBF in C26r. Given that all of the paleomagnetic studies on the ALG reveal reverse polarity remanence, C27n must have been missed by the

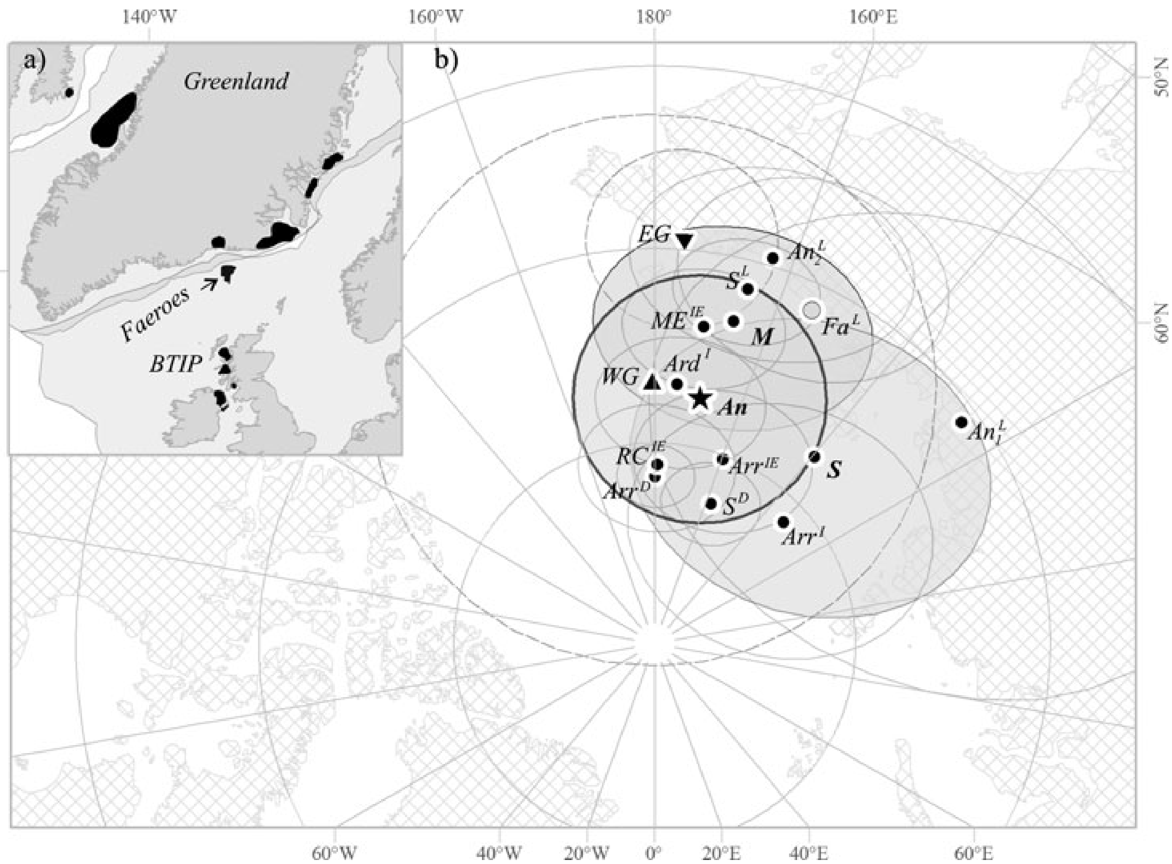

Figure 6. Selected paleomagnetic poles form the North Atlantic Igneous Province, (a) Greenland and its data are rotated 12.2° counter clockwise around an Euler pole at 48.3°N, 124.5°E into the Eurasian reference frame, interpolated between rotations for C25 (55.9 Ma) and C31 (67.7 Ma) of Gaina *et al*. (2002). Continent boundaries are taken from Gaina *et al.* (2009). Poles are symbolized as follows: background data set for BTIP and Faeroes = black and grey circles and grey hollow error ovals; New Mull, Skye and Antrim = stars and grey filled error ovals; West Greenland = upright triangles; East Greenland = inverted triangles, both with dashed error ovals. The abbreviations are listed in Table 3. The present day configuration of continents is shown with hatched filling.

paleomagnetic investigations or is simply missing from the geological record in the ALG. The interbasaltic hiatus is perhaps the obvious place to 'hide' C27n. The polarity of the field during emplacement of the Tardree rhyolite (Interbasaltic Formation) is uncertain because of its self-reversing property, but some of the results from site 13, in the rhyolite, suggest a reverse polarity. Wilson (1963) also report reverse polarities in the Tardree rhyolite. The polarity observed in the CM (also Interbasaltic Formation) is also reversed. The large thickness of laterite in the Interbasaltic represents enough time for the normal epoch ($61.65 - 61.983 = 0.333$ Ma) to remain unrecorded (see calculations above).

The accuracy of the $^{40}Ar/^{39}Ar$ method depends on precise and accurate age determination of primary and secondary standards. Because different investigations use different fluence monitors and/or different ages for the same monitor, a direct comparison of ages may be inappropriate. Therefore, to directly compare our $^{40}Ar/^{39}Ar$ ages with published ages from the NAIP we recalibrate the published ages relative to the primary standard GA-1550 and the secondary standard Fish Canyon sanidine according to Renne *et al.* (1998). We can then compare all ages with the global geomagnetic polarity time scale GTS2004 of Ogg & Smith (2004) which is calibrated to an age of 28.02 Ma for the Fish Canyon sanidine. To ease the comparison we only use recently published ages.

Even though Thompson (1985) reported a date of 61.6 Ma_R for the Tardree rhyolite in the ALG, the Vaigat Fm of Western Greenland, recording C27n (Riisager & Abrahamsen 1999), has been considered by some the oldest lava succession of the NAIP (Larsen *et al.* 1992; Chambers *et al.* 2005). The onset of emplacement of the lava piles elsewhere in the NAIP was believed to be contemporaneous with magnetochron C26r or younger (Fig. 7b; Table 4). This study verifies extrusion of the LBF in C27r, which makes them older than the Vaigat Fm (27n: Storey *et al.* 1998; Riisager & Abrahamsen 1999) and one of the oldest plateau lavas of the NAIP. Looking at the apparent ages of onset of volcanism across the BTIP on the map in Fig. 7, we notice a general northward younging of the major lava piles. However, the age of the oldest lavas on Skye is still not well constrained.

Paleoposition of the NAIP and the Plume Generation Zone hypothesis

Despite its success as a hypothesis, deep mantle plumes as an origin of LIP formation is controversial (Foulger *et al.* 2005). At the present day there exist two large low shear wave velocity (δV_s) provinces (LLSVP) in the deep mantle, namely the African (Fig. 8) and the almost antipodal Pacific LLSVP near the core–mantle boundary (CMB). They are recognized as the most prominent features in all global shear wave tomographic models and they are features that are isolated within the faster parts (subduction graveyards) of the deep mantle. Because LIPs move passively with the plates they reside on over geological timescales, Burke & Torsvik (2004) reconstructed 25 LIPs (Eldholm & Coffin 2000; Coffin *et al.* 2002)

Table 3. Selected paleomagnetic poles for the NAIP.

	SP	Unit	Label (°N)	sLat (°E)	sLong	*N*/*n*	*D*	*I*	*k*	α_{95} (°N)	pLat (°E)	pLong	dp	dm	A95
	British Isles	This study: Antrim, lavas & intrusives (1, 100 per cent, NA, NA)*	*An*	54.88	−6.09	37/305	181.3	−61.3	25.6	4.7	78.9	167.0	–	–	6.3
		Antrim, lavas (2, 100 per cent, 2496, 3)	An^{L}_{1}	55.10	−6.40	19/79	198.5	−59.7	11.5	10.3	71.0	125.8	12.1	13.6	-
		Antrim, lavas (3, 100 per cent, 3026, 2)	An^{L}_{2}	55.05	−6.05	25/–	184.7	−54.3	33.3	5.1	69.6	162.9	5.0	7.0	–
		Mull, lavas (4, 100 per cent, N/A, N/A)*	*M*	56.25	−6.10	26/319	182.9	−58.9	36.9	4.7	73.3	166.2	5.2	7.0	–
		Skye, lavas (5, 100 per cent, N/A, N/A*	*S*	57.42	−6.31		190.1	−64.8		5.7	77.7	145.4	7.4	9.2	–
		Skye, lavas (6, 100 per cent, 2506, 2)	S^{L}	57.40	−6.30	90/344	183.4	−58.4	35.8	2.5	71.5	165.2	2.8	3.8	–
		Skye, dykes (7, 80 per cent, 75, 2)	S^{D}	57.10	−5.90	409/1636	183.2	−67.1	–	1.5	82.5	158.0	2.1	2.5	–
		Arran, dykes (8, 82 per cent, 200, 2)	Arr^{D}	55.60	−5.20	413/-	179.0	−65.2	36.8	1.2	81.7	179.8	1.6	1.9	–
		Arran, intrusives (9, 40 per cent, 6090, 2,)	Arr^{I}	55.50	−5.20	10/100	8.8	66.2	104.6	4.7	81.2	133.2	6.3	7.7	–
		Arran, intrusives & extrusives (10, 75 per cent, 8718, 2)	Arr^{IE}	55.50	−5.20	165/-	183.7	−64.2	–	2.8	80.2	159.6	3.6	4.5	–
		Muck & Eigg igneous rocks (11, 97 per cent, 145, 3)	ME^{IE}	56.90	−6.20	133/524	181.0	−59.9	21.5	2.7	73.9	171.1	3.1	4.1	–
		Rhum & Canna, intrusives & extrusives (12, 95 per cent, 68, 2)	RC^{IE}	57.00	−6.50	107/445	178.7	−65.9	33.5	2.4	81.1	179.1	3.2	3.9	–
		Ardnamurchan, intrusives (13, 100 per cent, 146, 3)	Ard^{I}	56.70	−6.20	62/484	180.0	−63.0	–	2.7	77.0	175.0	3.3	4.2	–
	Fa	Faeroes, lavas (14, 70 per cent, 8901, 3)	Fa^{L}	61.90	−6.90	43/456	187.7	−60.9	24.5	4.5	71.4	154.7	–	–	6
		Comment	Label	–	–	N	–	–	K		pLat (°N)	pLong (°E)			
Means	WG	Lavas (15)	*WG*			5			30.1		76.9	180.4			14.2
	EG	Lavas, intrusives (15)	*EG*			6			197.4		69.4	176.1			4.8
	BTIP	Latest by us*				3			436.0		76.4	161.1			5.9
	BTIP	All				12			180.2		77.2	161.4			3.2
	NAIP	All				15			176.9		76.4	163.5			2.9

Note: SP, Sub-provinces, WG and EG are West and East Greenland, Rock unit: in parentheses, article reference number in list below, percentage of reversed, global database result ID, database demagnetization code; R, documented result. Label: Labels used in Fig. 6. Ages are from the following sources: Mull, Chambers & Pringle (2001); Antrim, this study; Skye, Bell & Williamson (2002); Arran/Muck/Eig/Rhum and Canna, Chambers *et al.* (2005); Faeroe Islands, Storey *et al.* (2007); sLat/sLong, study latitude/longitude; *N*/*n*, number of sites/samples; *D*/*I*, mean remanence declination/inclination; *k* and *K*, Fisher's (1953) precision parameter for the remanence and pole domain; α_{95} and A95: half angle of cone of 95 per cent confidence in the remanence and pole domain; plat/pLong: pole latitude/longitude; 60 Ma (°N and °E): Greenland poles rotated into pre-Atlantic positions with respect to Europe; dp/dm: semi axes of the ovals of 95 per cent confidence in pole positions. References for paleomagnetic data: (1) this study, (2) Løvlie *et al.* (1972), (3) Wilson (1970), (4) Ganerød *et al.* (2008), (5) Rousse *et al.* (in prep), (6) Wilson *et al.* (1972), (7) Wilson *et al.* (1982), (8) Dagley *et al.* (1978), (9) Mussett *et al.* (1987), (10) Hodgson *et al.* (1990), (11) Dagley & Mussett (1986), (12) Dagley & Mussett (1981), (13) Dagley *et al.* (1984), (14) Riisager *et al.* (2002), (15) mean poles from Ganerød *et al.* (2008). Poles marked with an asterisk are the latest contributions by the authors.

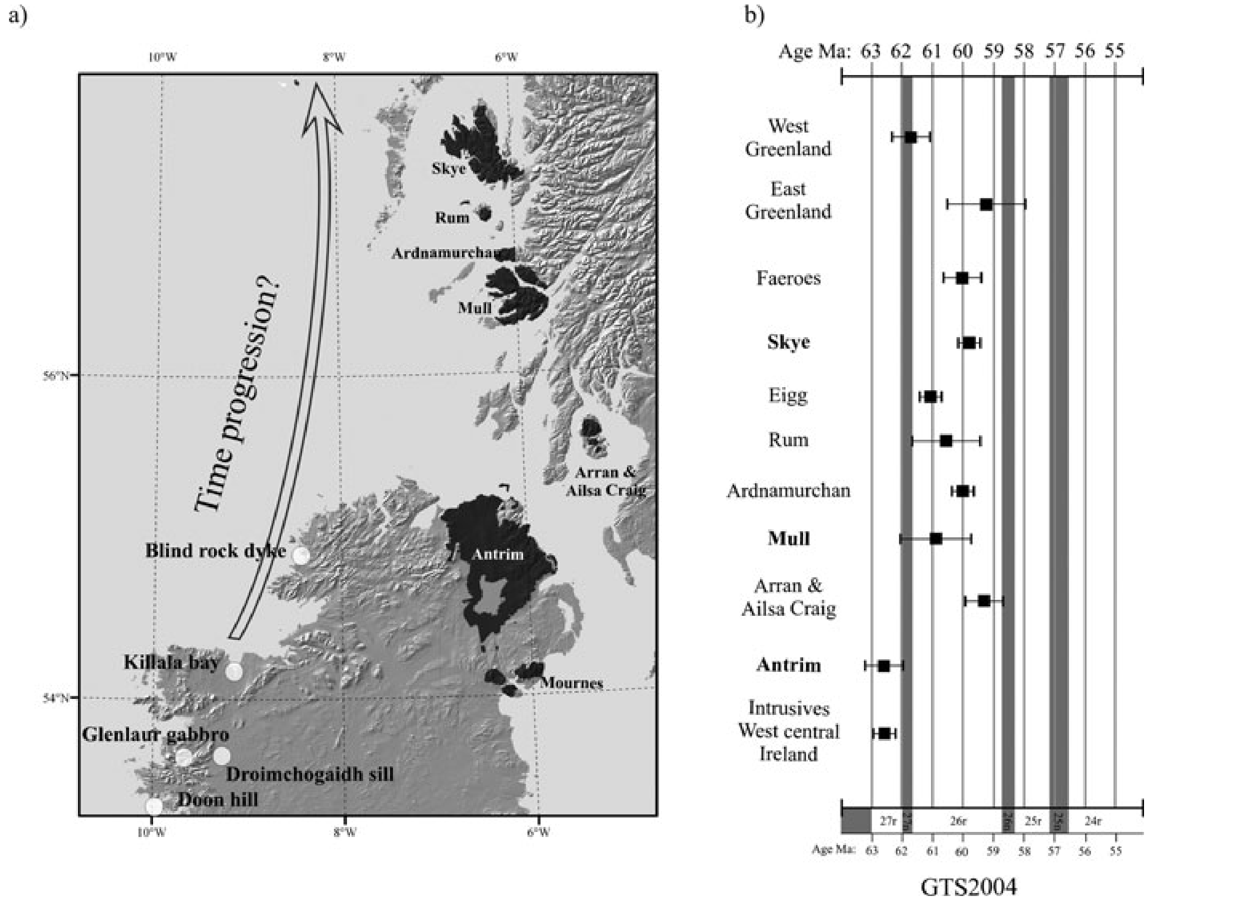

Figure 7. (a) Locations of the intrusive units dated by Thompson (1985) and (b) correlation across the BTIP and NAIP. Literature references can be found in Table 4. Error bars are at the 2σ level.

Table 4. Onset of magmatism across NAIP.

Subprovince	Name	Age reported	Recalculated age (2σ)
British Isles	Antrim (this study)	62.6 ± 0.31	62.6 ± 0.62
	West Central Ireland	61.97 ± 0.36	62.6 ± 0.36[b]
	Arran & Ailsa Craig	58.5 ± 0.6	59.35 ± 0.6[a]
	Mull	60.0 ± 0.5	60.88 ± 1.16[a]
	Ardnamurchan	59.14 ± 0.19	60.0 ± 0.38[a]
	Rum	60.1 ± 0.5	60.66 ± 1.0[c]
	Eigg	61.15 ± 0.25	61.15 ± 0.26
	Skye	58.91 ± 0.2	59.77 ± 0.4[a]
Faeroes	Lopra drill hole	60.1 ± 0.6	60.1 ± 0.6
East Greenland	Milne Land Fm	59.2 ± 1.4	59.2 ± 1.4
West Greenland	Vaigat Fm	60.3 ± 0.5	61.72 ± 0.5[d]

Notes: Both reported and recalculated ages are shown. Ages are calibrated to an age of 28.02 Ma for the Fish Canyon tuff and the references are as follows: Antrim, this study; West Central Ireland, Thompson (1985); Arran & Ailsa Craig, Ardnamurchan and Skye, Chambers (2000); Mull, Mussett (1986); Eigg, Hamilton *et al.* (1998); Faeroes and East Greenland, Storey *et al.* (2007) and Western Greenland, Storey *et al.* (1998). The indexes in the 'recalculated age' column shows which age for which monitor used in the recalculation and are as follows: (a) TC sanidine: 27.92 → 28.34 Ma, (b) B4 biotite: 17.19 → 17.37 Ma, (c) GA1550: 97.9 → 98.79 Ma and (d) FCT-3 biotite: 27.84 →28.19 Ma. New monitor ages are taken from Tables 2 and 3 in McDougall & Harrison (1999). All recalculated ages are shown with 2σ uncertainty. Eigg: Hamilton *et al.* (1998) overlaps with Chambers *et al.* (2005) and Storey *et al.* (2007). East Greenland: It is hard to judge the age plateaus of Hansen *et al.* (2002) due to high uncertainties on the $^{40}Ar/^{39}Ar$ intercepts. Isochrons overlaps with Storey *et al.* (2007). Southeast Greenland: the most reliable dates from Sinton & Duncan (1998) overlaps with Storey *et al.* (2007).

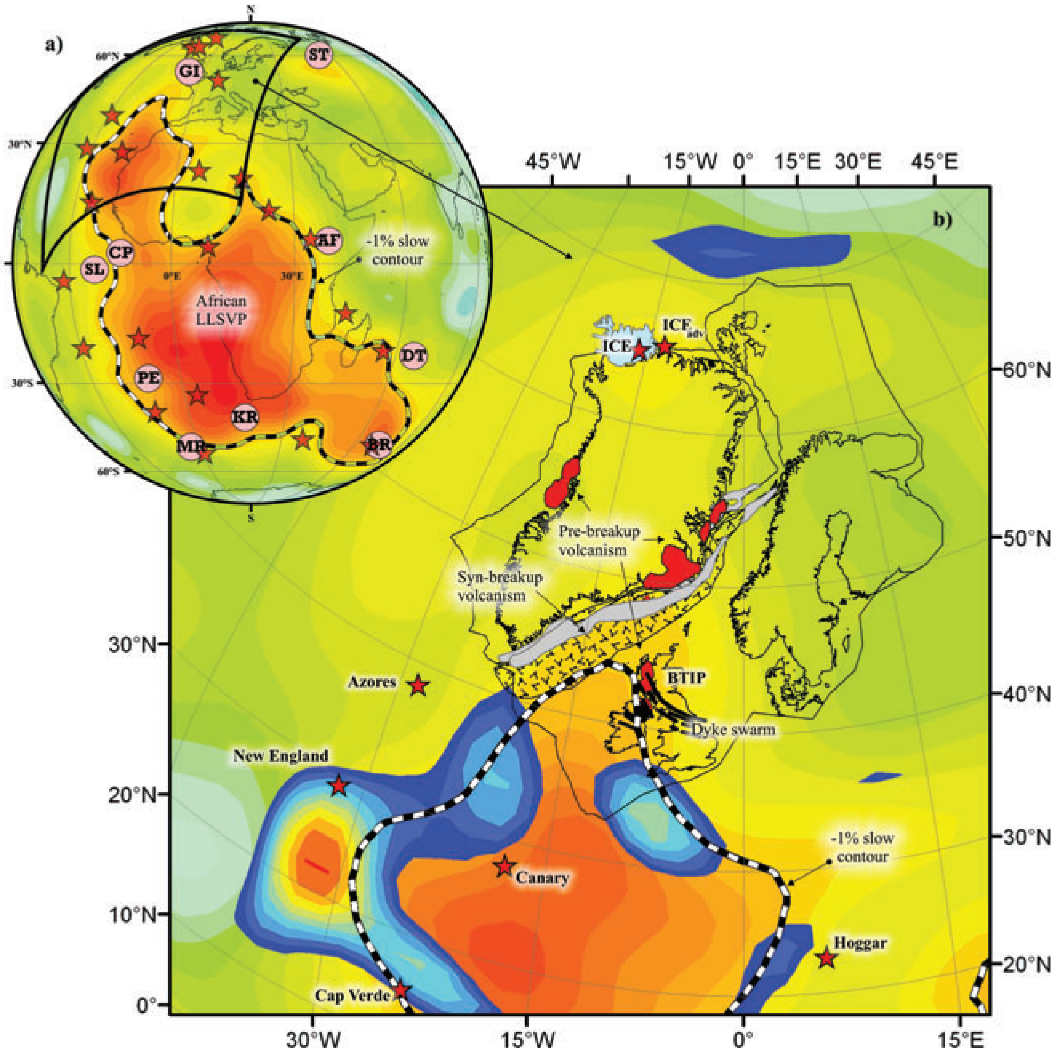

Figure 8. Reconstructed eruption sites for (a) selected LIPs (pink circles) according to a global paleomagnetic reference frame of Torsvik *et al.* (2006) with present day locations of hotspots (red stars) and (b) the NAIP from this study. Both (a) and (b) show the SMEAN tomography model (Becker & Boschi 2002), the 1 per cent slow shear wave velocity contour and the horizontal gradient over that contour as in Torsvik *et al.* (2006). Names of LIPs in (a) are labelled as follows: Greenland/Iceland = GI, Siberian Traps = ST, CAMP = CP, Sierra Leone = SL, Parana–Etendeka = PE, Afar = AF, Magellan = MR, Karroo = KR, Broken = BR, Deccan Traps = DT. The reconstruction in (b) is based on restoring Greenland to its 60 Ma position relative to Eurasia using same rotation parameters as in Fig. 6, and then rotating Eurasia and Greenland 13.6° clockwise around an Euler pole at 0°N, 73.5°E obtained from the mean of all NAIP poles in Table 3 (76.4°N, 163.5°E, A95 = 2.9).

to their original eruption sites with respect to the mantle. They then compared these eruption locations with different mantle tomography models and found a spatial match between downward projected eruption sites and the margins of the LLSVPs. Later, Torsvik *et al.* (2006) found a clear correlation between eruption sites of the past 200 Ma and that most LIPs (Fig. 8a) lay within ± 10° of the 1 per cent slow shear wave velocity contour in the SMEAN tomographic model (Becker & Boschi 2002). Apparently, these thermochemical LLSVPs (hotter and heavier) must have been resided there for at least 300 Ma (Torsvik *et al.* 2008a). The spatial correlation with the ‘Plume Generation Zones’ (Burke *et al.* 2008) indicates a deep plume origin for most LIPs, however, some outliers exist. The reconstructed NAIP in Torsvik *et al.* (2006) plot north of the 1 per cent slow shear wave velocity contour and correspond to a more diffuse part near the northern edge of the African LLSVP anomaly (Fig. 8a). To reconstruct NAIP the authors used several different reference frames.

Using the average paleomagnetic pole from the NAIP (76.4°N, 163.5°E, A95 = 2.9; Table 3), suggests that the NAIP erupted at a much lower latitude (50.5° for a coordinate coinciding with modern Reykjavik) than modern Iceland (64.1° for Reykjavik). Paleomagnetic data provide only latitudinal constraints, so theoretically there is a longitudinal degree of freedom of its position, however it has been shown by Torsvik *et al.* (2008b) that Eurasia has had insignificant cumulative longitudinal movement back to 100 Ma (approximately as stable as Africa used by Torsvik *et al.* (2008c) to construct their global reference frame).

As a sensitivity test, we also compared the paleolatitude for iceland at 60 Ma using the APWP for North-America and Europe (Torsvik *et al.* 2008c): the North-American APWP predicts a paleolatitude for a coordinate coinciding with Reykjavik of 50.2°, and the European APWP would give 53.2°, illustratiting that our result is within error of global paleomagnetic compilations. Invariably these show that the NAIP erupted at a latitude ∼1500 km south

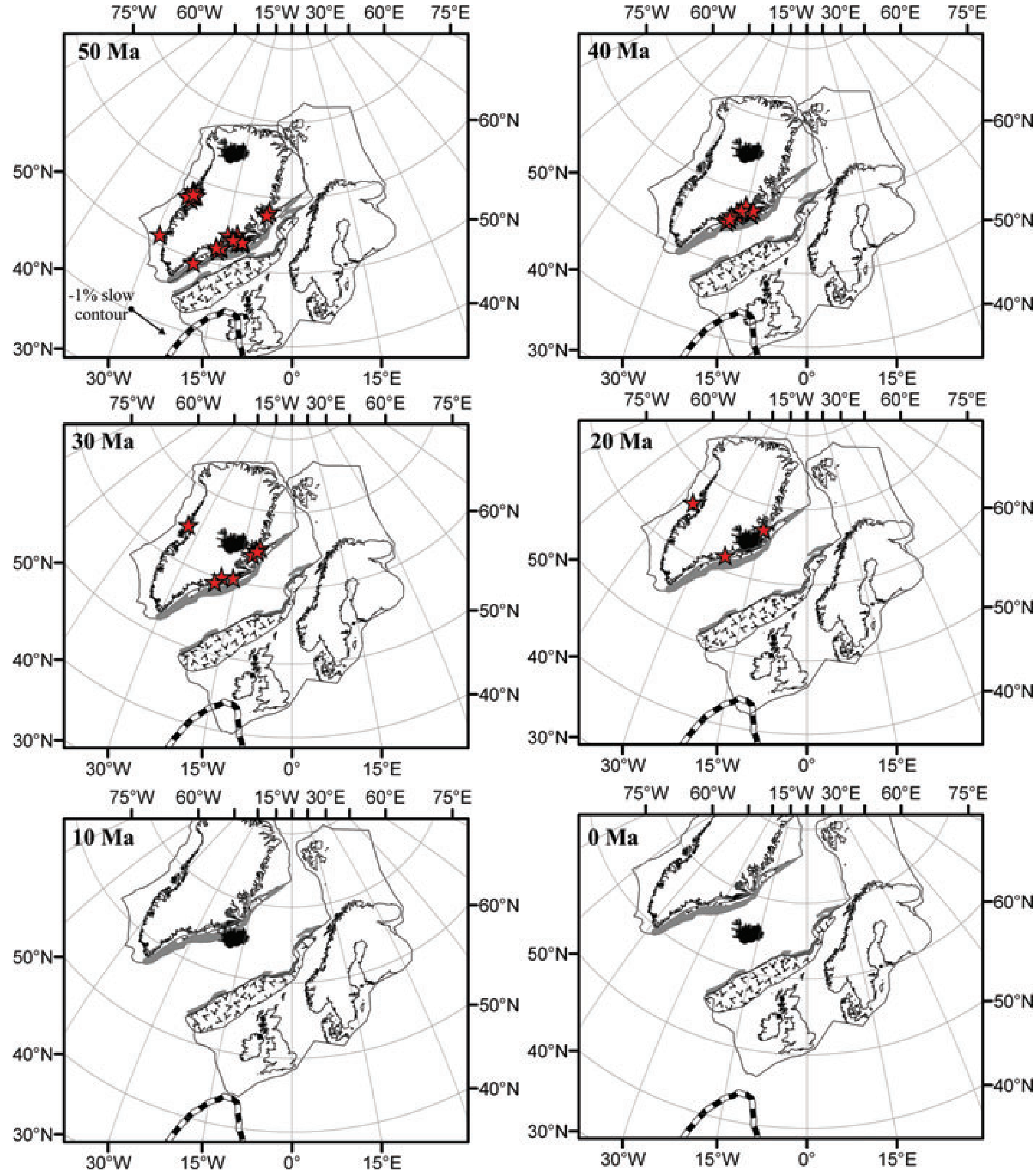

Figure 9. The NAIP through time, over a stationary Icelandic hotspot. Dated magmatic events are shown with a red star. Here, we first rotate Greenland (GR) to its position relative to a fixed Eurasia (EU) with a given time, rotation and Euler pole ^{GR}(°N, °E, rotation)^{EU} taken from Gaina *et al.* (2002), then restore it in a paleomagnetic reference frame (0°N, 73.5°E, rotation = 0.2267° per Ma). Restored eruption sites for the interval 60 – 50 Ma (Noble *et al.* 1988; Upton *et al.* 1995; Hirschmann *et al.* 1997; Price *et al.* 1997; Storey *et al.* 1998; Tegner *et al.* 1998; Larsen *et al.* 1999; Tegner & Duncan 1999; Lenoir *et al.* 2003) using rotations ^{GR}(53.17°N, 126.1°E, 10.01°)^{EU} then (0°N, 73.5°E, 11.3°), 50–40 Ma (Noble *et al.* 1988; Nevle *et al.* 1994; Tegner *et al.* 1998; Tegner & Duncan 1999; Lenoir *et al.* 2003) using rotations ^{GR}(60.9°N, 129.55°E, 8.31°)^{EU} then (0°N, 73.5°E, 9.1°), 40–30 Ma (Noble *et al.* 1988; Price *et al.* 1997; Storey *et al.* 1998) using rotations ^{GR}(68.34°N, 131.69°E, 7.04°)^{EU} then (0°N, 73.5°E, 6.8°), 30–20 Ma (Noble *et al.* 1988; Storey *et al.* 1998) using rotations ^{GR}(68.89°N, 132.51°E, 5.05°)^{EU} then (0°N, 73.5°E, 4.53°), 20–10 Ma using rotations ^{GR}(66.44°N, 132.98°E, 2.35°)^{EU} then (0°N, 73.5°E, 2.3°).

of its modern latitude. Our data thus confirm the APWP, and the reconstructed position of the NAIP plots close to the 1 per cent slow shear wave velocity contour previously termed the 'Plume Generation Zone' by Burke *et al*. (2008). However, this poses an important problem for the interpretation of the NAIP being generated from the Iceland hotspot, which is located ∼1500 km north of the NAIP eruption latitude. The reconstruction in Fig. 8b also shows different 60 Ma models of Iceland hotspot locations according to a fixed hotspot (Lawver & Müller 1994), shown with a label 'ICE', and a model of an advecting hotspot (ICE_{Adv}) according to Mihalffy *et al.* (2008) using the mantle convection model of Steinberger & O'Connell (1998). Both models plot far from the eruption sites according to our reconstruction. Any mismatch in position of the NAIP, and the back-projected position of the Iceland hotspot, if it is the cause of the NAIP, may not be significant given that the plume would have impacted the base of the lithosphere, spread out (Richards *et al.* 1989; Campbell & Griffiths 1990) and penetrated the lithosphere at weak points, such as the Great Glen Fault, Moine Thrust and Highland Boundary Fault in BTIP and the Ungava fault complex in Western Greenland. However, it would require a starting plume head of at least 2500 km in radius to reach the point where the first lavas (ALG) extruded, that is, twice the size of a starting plume head model of, that is Campbell & Griffiths (1990). Further, one would expect volcanism of similar age or older (>62–63 Ma) located closer to or above the projected position of the Icelandic hotspot (Fig. 8b). The later stage (55–56 Ma) assumed plume tail volcanism attributed to the volcanism in East Greenland (Tegner *et al.* 1998) would not either stem from the central axis (100 km wide) of the Icelandic hotspot.

We can see two ways of reconciling this paleolatitude problem: on the one hand, we may infer two separate hotspots; one plume located more to the south, at 60 Ma, responsible for the NAIP volcanism, and a separate plume or hotspot for the younger Icelandic hotspot for the last 20–30 Myr. In fact, the present day locations of nearby hotspots (i.e. Azores and Canary) are closer to the reconstructed BTIP (Fig. 8b), assuming that they have been fixed in the mantle back to 60 Ma. The assumed age of Azores hotspot is much younger than 60 Ma (Calvert *et al.* 2006; Hildenbrand *et al.* 2008) but seamounts around the Canary Islands have proven to be in the right time window (Geldmacher *et al.* 2005).

Alternatively, if the Iceland hotspot did create the NAIP, this hotspot must have gradually shifted northwards (moving hotspot), perhaps equivalent to the Hawaii-Emperor seamount chain, where the eruption latitudes were shown to shift significantly southwards over time (Tarduno *et al.* 2009). Current advection models (Steinberger & O'Connell 1998; Mihalffy *et al.* 2008), however, are not supporting this option.

The Greenland–Faeroe ridge has, by many, been attributed to a voluminous plume centred on the spreading ridge (White & Mackenzie 1989; Saunders *et al.* 1997; Storey *et al.* 2007). In Fig. 9, we show several time steps throughout the drift phase, which shows that the assumed Icelandic hotspot (fixed) would not interact with the East Greenland margin before 40–30 Ma, which violates a model in which the Greenland–Faeroe ridge represents a hotspot track. This age interval corresponds broadly in time with rift relocation (Kolbeinsey ridge) in the North Atlantic and rifting off the Jan Mayen microcontinent (Scott *et al.* 2005) from the East Greenland margin.

Whichever model will eventually arise to link the NAIP history to the Icelandic plume activity, it will have to take into account that during the ∼65 Ma to present volcanic history of the north Atlantic, the lithosphere underwent a ∼1500 km northward displacement, significantly challenging modern correlations.

CONCLUSION

This contribution presents a combined geochronologic and paleomagnetic investigation of the Antrim Lava Group. Despite its being the largest lava formation in the British Tertiary Igneous Province, little has been known about the timing of its emplacement. We have dated all three formations. Several samples from the Lower Basalt Formation give a weighed mean age of 62.6 ± 0.3 Ma (1σ, including 0.5 per cent error on the J-value). Further, we obtained an age of 61.3 ± 0.3 Ma for the stratigraphically higher Tardree rhyolite of the Interbasaltic Formation and an age of 59.6 ± 0.3 (1σ) for the Upper Basalt Formation. This constrains the nominal duration of emplacement of the Antrim Lava Group to be 3 ± 0.6 Ma (1σ). We also document a younger volcanism in the region at 49.9 ± 0.4 Ma.

Our reevaluation of the magnetic signature carried by the Antrim Lava Group confirms the presence of reverse polarity remanence in all three formations that corresponds to a ∼61 Ma paleomagnetic north pole position for Eurasia at latitude 78.9°N, longitude 167°E (A95 = 6.3). This is consistent with other paleomagnetic poles from the NAIP and in so doing confirms the paleomagnetic contiguity of the province at pre-north Atlantic breakup.

The radiometric ages documented herein span magnetochron C26r, C27n and C27r (GTS2004) meaning that a normal polarity chron was not detected in our paleomagnetic investigation, or that the chron is unrecorded in the Antrim Lava Group. The short normal chron most probably correlates in time with the Interbasaltic hiatus marked by laterites of the Interbasaltic Formation. This places the Lower Basalt Formation in magnetochron C27r and verifies that the basalts are older than the lowermost Vaigat Fm. of Western Greenland emplaced during Chron C27n. Looking at the apparent ages of onset of volcanism across the British Tertiary Igneous Province, we also notice a general northward younging of the major lava piles.

Our new paleomagnetic results provide a 60 Ma paleolatitudinal position of the NAIP in line with current apparent polar wander paths, and place it close to the 'Plume Generation Zone' (1 per cent slow shear wave velocity contour in the SMEAN tomographic model), from which previous studies document a spatial link with eruption sites for most large igneous provinces back to 300 Ma. Therefore, a deep mantle plume is a plausible cause for the NAIP volcanism. The paleolatitude of the NAIP, however, is ∼1500 km south of modern Iceland, challenging correlations of the NAIP to the Icelandic hotspot. We therefore speculate that the NAIP was either generated in a different, more southerly located early Palaeogene plume, or, alternatively, that the Icelandic plume migrated north. Future mantle modelling and a reevaluation of the Icelandic hostpot track will be required to reconcile this problem.

ACKNOWLEDGMENTS

MG would like to acknowledge the Norwegian Research Council and the Geological Survey of Norway for financial support, Elizabeth Eide for field support and ideas, the lab personnel at the NGU and NTNU, great help was given by Ian Mitchell and Derek Reay at the Geological Survey of Northern Ireland and Paul Lyle at the University of Ulster (Jordanstown, Belfast) during the initial stage of sampling. The authors appreciate the helpful and constructive reviews given by Leo Kirstjansson and Dennis Kent, and the editorial handling by Cor Langereis.

REFERENCES

Ade-Hall, J.M., Dagley, P., Wilson, R.L., Evans, A., Riding, A., Smith, P.J., Skelhorne, R. & Sloan, T., 1972. A palaeomagnetic study of the Mull regional dyke swarm, *Geophys. J. R. astr. Soc.,* **27,** 517–545.

Baksi, A.K., Archibald, D.A. & Farrar, E., 1996. Intercalibration of $^{40}Ar/^{39}Ar$ dating standards, *Chem. Geol.,* **129,** 307–324.

Becker, W. & Boschi, L., 2002. A comparison of tomographic and geodynamic mantle models, *Geochem. Geophys. Geosyst.,* **3**(1), 1003, doi:10.1029/2001GC000168.

Bell, B.R. & Williamson, I.T., 2002. Tertiary igneous activity, in *The Geology of Scotland*, pp. 371–407, ed. Trewin, N.H., The Geological Society of London, London.

Biggin, A., van Hinsbergen, D.J.J., Langereis, C.G., Straathof, G.B. & Deenen, M.H., 2008. Geomagnetic Secular variation in the Cretaceous Normal Superchron and in the Jurassic, *Phys. Earth Planet.,* **169,** 3–19.

Burke, K. & Torsvik, T.H., 2004. Derivation of large igneous provinces of the past 200 million years from long-term heterogeneities in the deep mantle, *Earth planet. Sci. Lett.,* **227,** 531–538.

Burke, K., Steinberger, B., Torsvik, T.H. & Smethurst, M.A., 2008. Plume generation zones at the margins of large low shear velocity provinces on the core–mantle boundary, *Earth planet. Sci. Lett.,* **265,** 49–60.

Butler, R.F., 1992. *Paleomagnetism: Magnetic Domains to Geologic Terranes*, p. 319, Blackwell Scientific Publications, Boston.

Calvert, A.T., Moore, R.B., McGeehin, J.P. & Rodrigues da Silva, A.M., 2006. Volcanic history and ^{40}Ar/^{39}Ar and ^{14}C geochronology of Terceira Island, Azores, Portugal, *J. Volc. Geotherm. Res.,* **156,** 103–115.

Campbell, I.H. & Griffiths, R.W., 1990. Implications of mantle plume structure for the evolution of flood basalts, *Earth planet. Sci. Lett.,* **99,** 79–93.

Chambers, L.M., 2000. Age and duration of the British Tertiary Igneous Province: implications for the development of the ancestral Iceland Plume, *PhD thesis*, University of Edinburgh, Edinburgh.

Chambers, L.M. & Pringle, M.S., 2001. Age and duration of activity at the Isle of Mull Tertiary igneous centre, Scotland, and confirmation of the existence of subchrons during Anomaly 26r, *Earth planet. Sci. Lett.,* **193,** 333–345.

Chambers, L.M., Pringle, M.S. & Parrish, R.R., 2005. Rapid formation of the Small Isles teritary centre constrained by precise ^{40}Ar/^{39}Ar and U-Pb ages, *Lithos*, **79,** 367–384.

Coffin, M.F., Pringle, M.S., Duncan, R.A., Gladczenko, T.P., Storey, M., Müller, R.D. & Gahagan, L.A., 2002. Kerguelen hotspot magma output since 130 Ma, *J. Petrol.,* **43,** 1121–1139.

Cooper, M.R., 2004. Palaeogene extrusive igneous rocks, in *The Geology of Northern Ireland, our Natural Foundation*, ed. Mitchell, W.I., pp. 167–178, 2nd edn, Geological Survey of Northern Ireland, Belfast.

Courtillot, V., Jaupart, C., Manighetti, I., Tapponnier, P. & Besse, J., 1999. On causal links between flood basalts and continental breakup, *Earth planet. Sci. Lett.,* **166,** 177–195.

Cox, A., 1969. Confidence limits for the precision parameter k. *Geophys. J. R. astr. Soc.,* **17,** 545–549.

Dagley, P. & Mussett, A.E., 1981. Palaeomagnetism of the British Tertiary igneous province: Rhum and Canna, *Geophys. J. R. astr. Soc.,* **65,** 475–491.

Dagley, P. & Mussett, A.E., 1986. Palaeomagnetism and radiometric dating of the British Tertiary igneous province: muck and Eigg, *Geophys. J. R. astr. Soc.,* **85,** 221–242.

Dagley, P., Mussett, A.E., Wilson, R.L. & Hall, J.M., 1978. The British Tertiary igneous province: palaeomagnetism of the Arran dykes, *Geophys. J. R. astr. Soc.,* **54,** 75–91.

Dagley, P., Mussett, A.E. & Skelhorn, R.R., 1984. The palaeomagnetism of the Tertiary igneous complex of Ardnamurchan, *Geophys. J. R. astr. Soc.,* **79,** 911–922.

Eldholm, O. & Coffin, M.F., 2000. The history and dynamics of global plate motions, in *Large Igneous Provinces and Plate Tectonics*, ed. Richards, M.A., Gordon, R.G. & van der Hilst, R.D., pp. 309–326, Geophysical Monograph, Vol. 121, American Geophysical Union, Washington, DC.

Fisher, R.A., 1953. Dispersion on a sphere. *Proc. R. Soc.,* **A217,** 295–305.

Fisher, N.I., Lewis, T. & Embleton, B.J.J., 1987. *Statistical Analysis of Spherical Data*, p. 329, Cambridge University Press, Cambridge.

Foulger, G.R., Natland, J.H., Presnall, D.C. & Anderson, D.L. (Eds.), 2005. Plates, Plumes, and Paradigms, 1 ed. The Geological Society of America, Special paper 388, Boulder, CO, USA.

Gaina, C., Roest, W.R. & Müller, R.D., 2002. Late Cretaceous-Cenozoic deformation of northeast Asia, *Earth planet. Sci. Lett.,* **197,** 273–286.

Gaina, C., Gernigon, L. & Ball, P., 2009. Paleocene-Recent Plate Boundaries in the NE Atlantic and the formation of Jan Mayen microcontinent, *J. geol. Soc. Lond.,* **166**, 601–616, doi:10.1144/0016-76492008-112.

Gamble, J.A., Wysoczanski, R.J. & Meighan, I.G., 1999. Constraints on the age of the British Tertiary Volcanic Province from ion microprobe U-Pb (SHRIMP) ages for acid igneous rocks from NE Ireland, *J. geol. Soc. Lond.,* **156,** 291–299.

Ganerød, M., Smethurst, M.A., Rousse, S., Torsvik, T.H. & Prestvik, T., 2008. Reassembling the Paleogene–Eocene North Atlantic igneous province: New paleomagnetic constraints from the Isle of Mull, Scotland, *Earth planet. Sci. Lett.,* **272,** 464–475.

Ganerød, M., Chew, D., Smethurst, M.A., Troll, V., Corfu, F., Meade, F. & Prestvik, T., 2010. Geochronology of the Tardree rhyolite complex, Northern Ireland: implications for the North Atlantic Igneous Province and zircon fission track and (U-Th)/He zircon studies, *Geology*, submitted.

Geldmacher, J., Hoernle, K., Bogaard, P. v. d., Duggen, S. & Werner, R., 2005. New ^{40}Ar/^{39}Ar age and geochemical data from seamounts in the Canary and Madeira volcanic provinces: Support for the mantle plume hypothesis, *Earth planet. Sci. Lett.,* **237,** 85–101.

Geological Survey of Northern Ireland, 1997. Northern Ireland, Solid Geology (Second edition). 1:250000. Keyworth, Nottingham, UK.

Gould, R., 2004. Antrim Lava Field: flow Patterns and Provenance of Interbasaltic Zircons, *PhD thesis*, University of Dublin, Dublin.

Hall, J.M., Wilson, R.L. & Dagley, P., 1977. A paleomagnetic study of the Mull lava succession, *Geophys. J. R. astr. Soc.,* **49,** 499–514.

Hamilton, M.A., Pearson, D.G., Thompson, R.N., Kelley, S.P. & Emeleus, C.H., 1998. Rapid eruption of Skye lavas inferred from precise U–Pb and Ar–Ar dating of the Rum and Cuillin plutonic complexes, *Nature*, **394,** 260–263.

Hildenbrand, A., Madureira, P., Marques, F.O., Cruz, I., Henry, B. & Silva, P., 2008. Multi-stage evolution of a sub-aerial volcanic ridge over the last 1.3 Myr: S. Jorge Island, Azores Triple Junction, *Earth planet. Sci. Lett*., **273,** 289–298.

Hill, I.G., Worden, R.H. & Meighan, I.G., 2000. Geochemical evolution of a palaeolaterite: the Interbasaltic Formation, Northern Ireland, *Chem. Geol.,* **166,** 65–84.

Hirschmann, M.M., Renne, P.R. & McBirney, A.R., 1997. ^{40}Ar/^{39}Ar dating of the Skaergaard intrusion, *Earth planet. Sci. Lett.,* **146,** 645–658.

Hodgson, B., Dagley, P. & Mussett, A.E., 1990. Magnetostratigraphy of the Tertiary igneous rocks of Arran, *Scott. J. Geol.,* **26,** 99–118.

Hospers, J. & Charlesworth, H.A.K., 1954. The natural permanent magnetization of the Lower basalts of Northern Ireland, *Mon. Not. R. astr. Soc. Geophys.,* **Suppl. 7,** 32–43.

Johnson, C.L., *et al*., 2008. Recent investigations of the 0–5 Ma geomagnetic field recorded by lava flows, *G-cubed*, **9,** Q04032.

Kent, J.T., Briden, J.C. & Mardia, K.V., 1983. Linear and planar structure in ordered multivariate data as applied to progressive demagnetisation of palaeomagnetic remanence, *Geophys. J. R. astr. Soc.,* **81,** 75–87.

King, S.D. & Anderson, D.L., 1998. Edge-driven convection, *Earth planet. Sci. Lett.,* **160,** 289–296.

Larsen, H.C. & Saunders, A.D., 1998. Tectonism and volcanism at the southeast Greenland rifted margin: A record of plume impact and later continental rupture, in *Proceedings of the Ocean Drilling Program, Scientific Results, 152*, pp. 503–533, ed. Saunders, A.D., Larsen, H.C. & Wise, S.W., College Station, TX (Ocean Drilling Program).

Larsen, L.M., Pedersen, A.K., Pedersen, G.K. & Piasecki, S., 1992. Timing and duration of Early Tertiary volcanism in the North Atlantic: new evidence from West Greenland, in *Magmatism and the Causes of Continental Break-Up*, pp. 321–333, ed. Storey, B.C., Alabaster, T. & Pankhurst, R.J., Geological Society Special Publication No. 68, London.

Larsen, L.M., Rex, D.C., Watt, W.S. & Guise, P.G., 1999. ^{40}Ar-^{39}Ar dating of alkali basaltic dykes along the southwest coast of Greenland; Cretaceous and Tertiary igneous activity along the eastern margin of the Labrador Sea, *Geol. Greenland Survey. Bull.,* **184,** 19–29.

Lawver, L.A. & Müller, R.D., 1994. Iceland hotspot track, *Geology*, **22,** 311–314.

Lenoir, X., Féraudc, G. & Geoffroy, L., 2003. High-rate flexure of the East Greenland volcanic margin: constraints from ^{40}Ar/^{39}Ar dating of basaltic dykes, *Earth planet. Sci. Lett.,* **214,** 515–528.

Løvlie, R., Gidskehaug, A. & Storetvedt, K.M., 1972. On the magnetization history of the Northern Irish basalts, *Geophys. J. R. astr. Soc.,* **27,** 487–498.

Lyle, P., 1980. A petrological and geochemical study of the Tertiary basaltic rocks of northeast Ireland, *J. Earth Sci., Dublin*, **2,** 137–152.

Mahoney, J.J., & Coffin, M.F., 1997. *Large Igneous Provinces: Continental, Oceanic, and Planetary Flood Volcanism*, 438 pp., Geophysical Monograph 100, American Geophysical Union, Washington, DC.

Manning, P.I., Robbie, J.A. & Wilson, H.E., 1960. Geology of Belfast and the Lagan Valley, *Memoir of the Geological Survey of Northern Ireland*, HMSO, Belfast.

McDougall, I. & Harrison, T.M., 1999. *Geochronology and Thermochronology by the ^{40}Ar/^{39}Ar method*, 2nd edn, Oxford University Press, New York.

McFadden, P.L., Merrill, R.T., McElhinny, M.W. & Sunhee L., 1991. Reversals of the earth's magnetic field and temporal variations of the dynamo families, *J. geophys. Res.,* **96,** 3923–3933.

McKenna, C., Gamble, J.A., Lyle, P. & Renne, P.R., 2009. New ^{40}Ar-^{39}Ar ages for lava flows and sills within the Antrim Lava Group, NE Ireland. *52nd Irish Geological Research Meeting*, Trinity College Dublin.

Meighan, I.G., McCormick, A.G., Gibson, D., Gamble, J.A. & Graham, I.J., 1988. Rb-Sr isotopic determinations and the timing of Tertiary central complex magmatism in NE Ireland, in *Early Tertiary Volcanism and the Opening of the NE Atlantic*, pp. 349–360, ed. Morton, A.C. & Parson, L.M., Geological Society London, Special Publications 39.

Meyer, R., van Wijk, J. & Gernigon, L., 2007. The North Atlantic Igneous Province: a review of models for its formation, in *Plates, Plumes, and Planetary Processes*, pp. 525–552, ed. Foulger, G.R. & Jurdy, D.M., Geological Society of America Special Paper 430.

Mihalffy, P., Steinberger, B. & Schmeling, H., 2008. The effect of the large-scale mantle flow field on the Iceland hotspot track, *Tectonophysics*, **447,** 5–18.

Mitchell, W.I., 2004. Cretaceous, in *The Geology of Northern Ireland, Our Natural Foundation*, pp. 149–160, ed. Mitchell, W.I., Geological survey of Northern Ireland, Belfast.

Mussett, A.E., 1986. ^{40}Ar-^{39}Ar step heating ages of the Tertiary igneous rocks of Mull, Scotland, *J. geol. Soc. Lond.,* **143,** 887–896.

Mussett, A.E., Dagley, P. & Skelhorn, R.R., 1980. Magnetostratigraphy of the Tertiary igneous succession of Mull, Scotland, *J. geol. Soc., Lond.,* **137,** 349–357.

Mussett, A.E., Dagley, P., Hodgson, B. & Skelhorn, R.R., 1987. Palaeomagnetism and age of the quartz-porphyry intrusions, Isle of Arran, *Scott, J. Geol.,* **23,** 9–22.

Nevle, R.J., Brandriss, M.E., Bird, D.K., McWilliams, M.O. & O'Neil, J.R., 1994. Tertiary plutons monitor climate change in East Greenland, *Geology*, **22,** 775–778.

Nier, A.O., 1950. A redetermination of the relative abundances of the isotopes of carbon, nitrogen, oxygen, argon, and potassium, *Phys. Rev.,* **77,** 789–793.

Noble, R.H., Macintyre, R.M. & Brown, P.E., 1988. Age constraints on Atlantic evolution: timing of magmatic activity along the E Greenland continental margin, in *Early Tertiary Volcanism and the Opening of the NE Atlantic*, Special Publications 39, pp. 201–214, eds Morton, A.C. & Parson, L.M., Geological Society, London, UK.

O'Connor, J.M., Stoffers, P., Wijbrans, J.R., Shannon, P.M. & Morrissey, T., 2000. Evidence from episodic seamount volcanism for pulsing of the Iceland plume in the past 70 Myr, *Nature*, **408,** 954–958.

Ogg, J.G. & Smith, A.G., 2004. The geomagnetic polarity time scale, in *A Geologic Time Scale 2004*, pp. 63–86, ed. Gradstein, F.M., Ogg, J.G. & Smith, A.G., Cambridge University Press, Cambridge, UK.

Old, R.A., 1975. The age and field relationships of the Tardree Tertiary rhyolite complex, County Antrim, N. Ireland, *Bull. geol. Surv. G. B.,* **51,** 21–40.

Pillans, B., 1997. Soil development at snail's pace: evidence from a 6 Ma soil chronosequence on basalt in north Queensland, Australia, *Geoderma*, **80,** 117–128.

Price, S., Brodie, J., Whitham, A. & Kent, R., 1997. Mid-Tertiary rifting and magmatism in the Trail region, East Greenland, *J. geol. Soc. Lond.,* **154,** 419–434.

Renne, P.R., Swisher, C.C., Deino, A.L., Karner, D.B., Owens, T.L. & DePaolo, D.J., 1998. Intercalibration of standards, absolute ages and uncertainties in ^{40}Ar/^{39}Ar dating, *Chem. Geol.,* **145,** 117–152.

Richards, M.A., Duncan, R.A. & Courtillot, V., 1989. Flood basalts and hot spot tracks: Plume heads and tails, *Science*, **246,** 103–107.

Riisager, P. & Abrahamsen, N., 1999. Magnetostratigraphy of Palaeocene basalts from the Vaigat Formation of West Greenland, *Geophys. J. Int.,* **137,** 774–782.

Riisager, P., Riisager, J., Abrahamsen, N. & Wagstein, R., 2002. New paleomagnetic pole and magnetostratigraphy of Faroe Islands flood volcanics, North Atlantic igneous province, *Earth planet. Sci. Lett.,* **201,** 261–276.

Riisager, J., Riisager, P. & Pedersen, A.K., 2003a. The C27n-C26r geomagnetic polarity reversal recorded in the west Greenland flood basalt province: How complex is the transitional field? *J. geophys. Res.,* **108,** doi:10.1029/2002JB002124.

Riisager, J., Riisager, P. & Pedersen, A.K., 2003b. Paleomagnetism of large igneous provinces: case-study from West Greenland, North Atlantic igneous province, *Earth planet. Sci. Lett.,* **214,** 406–425.

Saunders, A.D., Fitton, J.G., Kerr, A.C., Norry, M.J. & Kent, R.W., 1997. The North Atlantic igneous province, in *Large Igneous Provinces*, pp. 45–93, ed. Mahoney, J.J., Coffin, M.F., Geophysical Monograph 100, American Geophysical Union, Washington, DC.

Scott, R.A., Ramsey, L.A., Jones, S.M., Sinclair, S. & Pickles, C.S., 2005. Development of the Jan Mayen microcontinent by linked propagation and retreat of spreading ridges, in *Onshore–offshore relationships on the North Atlantic Margin*, pp. 69–82, ed. Wandas, B.E.A., Norwegian Petroleum Society Special Publication, Amsterdam.

Simms, M.J., 2000. The sub-basaltic surface in northeast Ireland and its significance for interpreting the Tertiary history of the region, *Proc. Geologists' Assoc.,* **111,** 321–336.

Sinton, C.W. & Duncan, R.A., 1998. ^{40}Ar-^{39}Ar ages of lavas from the Southeast Greenland margin, ODP Leg 152 and the Rockall Plateau, DSDP Leg 81, in *Proceedings of the Ocean Drilling Program, scientific results, 152*, pp. 387–402, ed. Saunders, A.D., Larsen, H.C. & Wise, W., Ocean Drilling Program, College Station, Texas.

Steiger, R.H. & Jäger, E., 1977. Subcommission on geochronology: convention on the use of decay constants in geo- and cosmochronology, *Earth planet. Sci. Lett.,* **36,** 359–362.

Steinberger, B. & O'Connell, R., 1998. Advection of plumes in mantle flow: implications for hotspot motion, mantle viscosity and plume distribution, *Geophys. J. Int.,* **132,** 412–434.

Storey, M., Duncan, R.A., Pedersen, A.K., Larsen, L.M. & Larsen, H.C., 1998. ^{40}Ar/^{39}Ar geochronology of the West Greenland Tertiary volcanic province, *Earth planet. Sci. Lett.,* **160,** 569–586.

Storey, M., Duncan, R.A. & Tegner, C., 2007. Timing and duration of volcanism in the North Atlantic Igneous Province: implications for geodynamics and links to the Iceland Hotspot, *Chem. Geol.,* **241,** 264–281.

Tarduno, J.A., Bunge, H.-P., Sleep, N.H. & Hansen, U., 2009. The bent Hawaiian-Emperor hotspot track: inheriting the mantle wind, *Science*, **324,** 50–53.

Tauxe, L. & Kent, D.V., 2004. A simplified statistical model for the geomagnetic field and the detection of shallow bias in paleomagnetic inclinations: Was the ancient magnetic field dipolar?, in *Timescales of the Paleomagnetic Field*, pp. 101–116, ed. Channel, J.E.T., Kent, D.V., Lowrie, W. & Meert, J.G., Geophysical Monograph 145, American Geophysical Union, Washington, DC.

Tauxe, L., Kodama, K.P. & Kent, D.V., 2008. Testing corrections for paleomagnetic inclination error in sedimentary rocks: a comparative approach, *Phys. Earth planet Inter.,* **169,** 152–165.

Tegner, C. & Duncan, R.A., 1999. ^{40}Ar-^{39}Ar chronology for the volcanic history of the southeast Greenland rifted margin, *Proc. ODP Sci. Res.,* **163,** 53–62.

Tegner, C., Duncan, R.A., Bernstein, S., Brooks, C.K., Bird, D.K. & Storey, M., 1998. ^{40}Ar/^{39}Ar geochronology of Tertiary mafic intrusions along the East Greenland rifted margin: relation to flood basalts and the Iceland hotspot track, *Earth planet. Sci. Lett.,* **156,** 75–88.

Théveniaut, H. & Freyssinet, P., 1999. Paleomagnetism applied to lateritic profiles to assess saprolite and duricrust formation processes: the example of Mont Baduel profile (French Guiana), *Palaeogeogr. Palaeoclimatol. Palaeoecol*., **148,** 209–231.

Thompson, S.J., 1979. Preliminary report on the ballymacilroy No. 1 borehole, Ahoghill, Co. Antrim, Open File Report no. 63, Geological Survey of Northern Ireland, Belfast.

Thompson, P., 1985. Dating the British Tertiary Igneous Province in Ireland by the ^{40}Ar-^{39}Ar stepwise Degassing Method, *PhD thesis*, University of Liverpool, Liverpool.

Torsvik, T.H., Briden, J.C. & Smethurst, M.A., 2000. Super-IAPD Interactive analysis of palaeomagnetic data, www.geodynamics.no/Web/Content/Software/, 2009.

Torsvik, T.H., Müller, R.D., Van Der Voo, R., Steinberger, B. & Gaina, C., 2008c. Global plate motion frames: toward a unified model, *Rev. Geophys.,* **46,** RG3004.

Torsvik, T.H., Smethurst, M.A., Burke, K. & Steinberger, B., 2006. Large igneous provinces generated from the margins of the large low-velocity provinces in the deep mantle, *Geophys. J. Int.,* **167,** 1447–1460.

Torsvik, T.H., Smethurst, M.A., Burke, K. & Steinberger, B., 2008a. Long term stability in deep mantle structure: evidence from the ∼300 Ma Skagerrak-Centered Large Igneous Province (the SCLIP), *Earth planet. Sci. Lett.,* **267,** 444–452.

Torsvik, T.H., Steinberger, B., Cocks, L.R.M. & Burke, K., 2008b. Longitude: linking Earth's ancient surface to its deep interior, *Earth planet. Sci. Lett.,* **276,** 273–282.

Upton, B.G.J., Emeleus, C.H., Rex, D.C. & Thirlwall, M.F., 1995. Early Tertiary magmatism in NE Greenland, *J. geol. Soc. Lond.,* **152,** 959–964.

Vandamme, D., 1994. A new method to determine paleosecular variation, *Phys. Earth planet Inter.,* **85,** 131–142.

Wakatsuki, T. & Rasyidin, A., 1992. Rates of weathering and soil formation, *Geoderma*, **52,** 251–263.

Walker, G.P.L., 1959. Some observations on the Antrim basalts and associated dolerite intrusions, *Proc. Geol. Assoc.,* **70,** 179–205.

White, N. & Lovell, B., 1997. Measuring the pulse of a plume with the sedimentary record, *Nature*, **387**(6636), 888–891.

White, R. & Mackenzie, D., 1989. Magmatism at rift zones: the generation of volcanic continental margins and flood basalts, *J. geophys. Res.,* **94,** 7685–7729.

White, A.F., Blum, A.E., Schulz, M.S., Vivit, D.V., Stonestrom, D.A., Larsen, M., Murphy, S.F. & Eberl, D., 1998, Chemical weathering in a tropical watershed, Luquillo Mountains, Puerto Rico: I. Long-term versus short-term weathering fluxes, *Ceochim. Cosmochim. Acta*, **62,** 209–226.

Wilson, R.L., 1963. The palaeomagnetism of some rhyolites from Northern Ireland, *Geophys. J. R. astr. Soc.,* **8,** 235–241.

Wilson, R.L., 1970. Palaeomagnetic stratigraphy of Tertiary lavas from Northern Ireland, *Geophys. J. R. astr. Soc.,* **20,** 1–9.

Wilson, H.E., & Manning, P.I., 1978. Geology of the Causeway Coast (2 volumes), *Memoir of the Geological Survey of Northern Ireland*, sheet 7.

Wilson, R.L., Dagley, P. & Ade-Hall, J.M., 1972. Palaeomagnetism of the British Tertiary igneous province: the Skye lavas, *Geophys. J. R. astr. Soc.,* **28,** 285–293.

Wilson, R.L., Hall, J.M. & Dagley, P., 1982. The British Tertiary Igneous Province: palaeomagnetism of the dyke swarm along the Sleat coast of Skye, *Geophys. J. R. astr. Soc.,* **68,** 317–323.

SUPPORTING INFORMATION

Additional Supporting Information may be found in the online version of this article:

The accompanying pages include raw ^{40}Ar/^{39}Ar heating experiment data and inverse isochron analysis.
Table S1. Raw ^{40}Ar/^{39}Ar step heating data.
Figure S1. Inverse isochron analysis.

Please note: Wiley-Blackwell are not responsible for the content or functionality of any supporting materials supplied by the authors. Any queries (other than missing material) should be directed to the corresponding author for the article.